Routing in Sparse Vehicular Ad Hoc Wireless Networks

Nawaporn Wisitpongphan, Fan Bai, Priyantha Mudalige, Varsha Sadekar, and Ozan Tonguz

Derived from experiment

***Abstract*— A Vehicular Ad Hoc Network (VANET) may exhibit a bipolar behavior, i.e., the network can either be fully connected or sparsely connected depending on the time of day or on the market penetration rate of the wireless communication devices. In this paper, we use empirical vehicle traffic data measured on I-80 freeway in California to develop a comprehensive analytical framework to study the disconnected network phenomenon and its network characteristics. These characteristics shed light on the key routing performance metrics of interest in disconnected VANETs, such as the average time taken to propagate a packet to disconnected nodes (i.e., the *re-healing time*).**

Our results show that, depending on the sparsity of vehicles or the market penetration rate of cars using Dedicated Short Range Communication (DSRC) technology, the network re-healing time can vary from a few seconds to several minutes. This suggests that, for vehicular safety applications, a new ad hoc routing protocol will be needed as the conventional ad hoc routing protocols such as Dynamic Source Routing (DSR) and Ad Hoc On-Demand Distance Vector Routing (AODV) will not work with such long re-healing times. In addition, the developed analytical framework and its predictions provide valuable insights into the VANET routing performance in the disconnected network regime.

***Index Terms*— Routing, vehicular ad hoc Networks, broadcasting, vehicle traffic modeling.**

I. Introduction

VERY MUCH different from conventional ad hoc wireless networks [1], a VANET not only experiences rapid changes in wireless link connections, but may also have to deal with different types of network densities. For example, VANETs on freeways or urban areas are more likely to form highly dense networks during bumper-to-bumper rush hour traffic, while VANETs are expected to experience frequent network fragmentation in sparsely populated rural freeways or during late night hours. Until now, most of VANET research has focused on analyzing routing algorithms to handle the *broadcast storm* problem in a highly dense network topology [2], [3], under the over-simplified assumption that a typical VANET is a well-connected network in nature. In contrast, we believe that the *disconnected network* problem is also a crucial research challenge for developing a reliable and efficient routing protocol that can support highly diverse network topologies.

Manuscript received February 1, 2007; revised June 29, 2007.

Nawaporn Wisitpongphan and Ozan Tonguz are with Carnegie Mellon University, ECE Dept., Pittsburgh, PA 15213-3890, USA (e-mail: {nawaporn,tonguz}@ece.cmu.edu

Fan Bai, Priyantha Mudalige, and Varsha Sadekar are with General Motors Corporation, ECI Lab, Warren, MI 48092, USA (e-mail: {fan.bai,priyantha.mudalige,varsha.k.sadekar}@gm.com).

Digital Object Identifier 10.1109/JSAC.2007.071005.

In particular, we are interested in answering the following three questions:

1) Is the network disconnection problem a severe problem prohibiting vehicles from successfully delivering safety messages to other vehicles?
2) What are the key characteristics of the network disconnection in VANETs and how do they affect the network performance?
3) How can we solve or mitigate this disconnected VANET problem?

With a deeper understanding toward the key characteristics of network disconnection, our objective is not only to demonstrate that network fragmentation is a fundamental routing issue that needs to be addressed in vehicular ad hoc networks research, but also to shed light on some of the potential solutions (e.g., the "store-carry-forward" mechanism [4]).

To answer these three questions, in this paper, we develop a comprehensive analytical framework built upon an extended *car following model* to investigate the major characteristics of disconnected VANETs. First, we examine the key parameters of vehicle traffic model (i.e., inter-arrival time and inter-vehicle spacing between vehicles on the road, etc.) by analyzing the empirical data collected from a dual-loop detector along the I-80 freeway on June 27, 2006. Interestingly, we observe that inter-vehicle spacing follows an *exponential distribution* as long as the effective traffic volume, i.e., density of the equipped vehicles, is less than 1000 veh/hr. Using the measured data, our results show that the probability of network disconnection, even with 100% market penetration, is up to 35% on an I-80 Freeway during late night hours, while vehicles form a well-connected network during rush-hour. With a small market penetration rate, however, the disconnected network pheonomenon can be observed even during rush hours [5].

To better understand the impact of vehicle mobility and traffic density on network disconnection, we propose a novel analytical framework to capture several major characteristics of network disconnection, including probability of being disconnected from the following vehicle, cluster size, cluster lengths, intra- and inter-cluster spacing. Our Monte-Carlo simulations demonstrate that the predictions of the developed analytical framework perfectly match the simulation results, further validating our analytical framework. Besides these metrics, we also explore another dynamic characteristic, the *re-healing time*. This metric, which represents the minimal delay of packet delivery between a source and a destination using both direct wireless transmissions (when a network is well-connected) and indirect packet relays via the opposite-

direction vehicles (when a network is fragmented), is critical to vehicular safety applications because many of them are delay-sensitive. Our simulation results show that the total end-to-end packet delay on a 10 km freeway segment is less than 2 minutes even when the effective traffic volume is very low. Here, the average re-healing time that relay vehicle experiences is, on average, less than 30 seconds. These results suggest that while conventional routing protocols such as AODV or DSR may not be suitable for long-delay scenarios caused by network fragmentation, the "store-carry-forward" mechanism is a feasible solution for non-critical traffic efficiency applications in a sparsely populated network [4]. The key contributions of our study can be summarized as follows:

1) Characterizing the probability distribution of *inter-arrival time* and *inter-vehicle spacing* between vehicles on freeways by using empirical data from a realistic traffic environment. This leads to the observation that inter-arrival time and inter-vehicle spacing can be reasonably approximated by *exponential distributions* when the network is fragmented. Also, the empirical data verifies our conjecture that VANETs may experience network fragmentation because of vehicle traffic sparsity and low market penetration of wireless devices.
2) Developing a comprehensive analytical framework that sheds light on major characteristics of VANETs, which helps to better understand the behavior of disconnected VANETs under various traffic densities and mobility scenarios. In particular, we explore and quantify the metric of re-healing time, quantifying the average delay needed to deliver messages between disconnected vehicles, which is the main focus of many vehicular active safety applications.
3) Suggesting a potential routing solution (i.e., "store-carry-forward") for disconnected VANETs problem. In particular, we show, via extensive Monte Carlo simulations, that by using both store-carry-forward and a simple broadcast mechanisms in a disconnected VANET, the average network re-healing time (on a per-hop basis) is on the order of a few to several seconds.

The remainder of this paper is organized as follows. In Section II, we discuss the related work. The background on the lane-level traffic model is provided in Section III, along with the proposed road-level traffic model. In Section IV, we develop an analytical traffic model which we later use to construct a comprehensive analytical framework to study disconnected VANETs in Section V and Section VI. Simulation results and a discussion are presented in Section VII. Finally, we conclude our study in Section VIII, while the necessary auxiliary material is relegated to the Appendices.

II. Related Work

In our study, the proposed vehicular mobility model is directly derived from *empirical data* collected in a real-world environment. While there are several existing traffic models, most of them are only suitable for simulation studies and are not mathematically tractable. For example, the Random Waypoint (RWP) model was proposed as a generic mobility model for network simulations [6], where mobile nodes randomly select destinations with a randomly chosen velocity. However, such a simplified mobility model cannot capture many rich characteristics of the real vehicular traffic. Consequently, Reference Point Group Mobility (RPGM) was introduced to emulate grouping behavior of battlefield scenarios [7]; Freeway/Manhattan model captured the impact of geographic restriction (i.e., road) on vehicular mobility [8]; Simplified car-following model is used to restrict vehicular movements on a road at a lane-level defined by real map data [9]. However, in most cases, the over-simplified assumptions necessary to make the analysis tractable often result in models that fail to adequately represent the extreme complexity of the real-world mobility patterns. In [10], the authors introduce a very detailed analytical two-lane traffic model which can be efficiently used for simulation purposes, but the model seems too complicated and is not suitable for our study. Moreover, unlike most studies which concentrate on evaluating the impact of mobility models on MANET routing protocols in well-connected scenarios [3], [11], we emphasize the fact that VANETs are prone to network fragmentation due to the uneven nature of vehicle traffic and market penetration.

Apart from mobility modeling, the emerging field of Delay Tolerant Networks (DTN)is also synergistic with the problem formulation of disconnected VANETs. The DTN framework [12] is proposed to analyze and interconnect challenged networks where end-to-end routes between mobile nodes may not exist, such as in wildlife tracking sensor networks, interplanetary networks, and military ad hoc networks. In such challenged networks, traditional MANET routing protocols such as DSR [13] or AODV [14] would not work well. Instead, an asynchronous message forwarding paradigm based on *store-carry-forward* concept is used to achieve interoperability among different challenged networks [12], [15]. A number of routing protocols specifically designed to cope with routing in sparsely connected Mobile Ad hoc Networks that fall into the generic framework of Delay Tolerant Networks are as follows: DataMules [16] are mobile messengers which promote the network connectivity in a sensor network by providing access between the virtual backbone and sensor nodes; Epidemic routing relies on mobile nodes to exchange the data they possess whenever they encounter new neighbors [17]; Role-based multicast approach is proposed to achieve maximum reachability in a sparsely connected or fragmented network by using the *store-carry-forward* mechanism [18]; Single-copy [19] and Multi-copy 'Spray and Wait' [20] are shown to be efficient alternatives for message delivery. However, most of these studies focused on 2-dimensional topology with random way point model where node mobility has less real-world restrictions. Unlike previous studies, we focus on network fragmentation scenarios in VANETs with *realistic vehicular mobility models*. Also, our main objective in this paper is to establish a comprehensive analytical framework for understanding the fundamental characteristics of disconnected VANETs in addition to studying the feasibility of the *store-carry-forward* approach. We believe that a deeper understanding will facilitate the design of efficient and robust message delivery protocols in intermittently connected VANETs.

Although there are a few studies that address similar routing issues in sparsely connected VANETs, this paper, to the

best of our knowledge, is the first comprehensive research effort to characterize key routing parameters in intermittently connected or disconnected VANETs by using experimental, analytical, and simulation-based studies. In particular, in addition to the pioneering study by [21] which also focuses on exploring the feasibility of the *store-carry-forward* concept on a bidirectional highway via extensive simulations, we have developed a comprehensive *analytical framework* which can be used to derive several network characteristics and key routing performance metrics such as per-hop delay (re-healing time) in sparsely connected VANETs.

While our work only focuses on a sparsely connected highway network, some researchers have looked into a sparsely connected VANET with a Manhattan Grid model. The proposed techniques to disseminate information in such a scenario include disseminating the packet into different directions when passing by the intersections [22], relying on fixed infrastructures to provide network connectivity [11], or using GPS and map information to determine whom to forward the packet to [23]. These 2-D Manhattan Grid studies are complementary to the problem of disconnected VANET in a 1-D Highway scenario, investigated in this paper.

III. Vehicle Traffic Model

In this section, building upon a well-known traffic model in civil engineering, we propose a parameterized traffic model to capture the real vehicular mobility behavior. In the next section, we apply this model to characterize the vehicular traffic behavior.

Car following model is used in civil engineering to describe traffic behavior on a *single-lane* under both free-flow and congested traffic conditions. This model assumes that each driver in the following vehicle maintains a safe distance from the leading vehicle and the deceleration factor is also taken into account for the braking performance and drivers' behavior. The complete mathematical model is given by

$$S' = L + \beta' V + \gamma V^2 \tag{1}$$

where S' is the headway spacing between rear bumper to rear bumper, L is the effective vehicle length in meters, and V is the vehicle speed in meters/second. β' is driver reaction time in seconds, and γ coefficient is the reciprocal of twice the maximum average deceleration of a following vehicle (i.e., approximately 0.075 s^2/m). In particular, γ factors in the differences in the braking performances between leading and following vehicles. Both β' parameter and γ coefficient are introduced to ensure sufficient spacing so that following vehicle can come to a complete stop if the leading vehicle suddenly brakes. As in many other civil engineering studies, we use a so-called "good driving" rule which assumes that each vehicle has similar braking performance (i.e., $\gamma \approx 0$). In this case, the car following model can be simplified as

$$S' = L + \beta' V. \tag{2}$$

While the car following model is one of the most popular models in civil engineering, it has some limitations in modeling freeway traffic behavior for the purpose of wireless networking research, which can be summarized as follows:

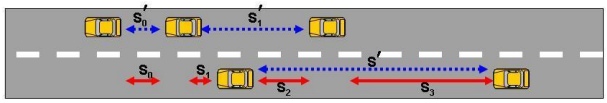

Fig. 1. Comparison of Lane-level and Road-level spacing.

1) Car following model describes headway spacing between two adjacent vehicles of the same lane (i.e., **lane-level spacing**), which is the focus of many studies in civil engineering. From the network connectivity standpoint, however, we observe that the most relevant metric is spacing from leading vehicle to the nearest following vehicle on a multi-lane road (i.e., **road-level spacing**), regardless of whether the following vehicle is on the same lane or on a different lane from the leading vehicle. This metric plays an important role in determining the network connectivity, simply because the distance to the nearest neighbor decides whether a wireless link between vehicles exists or not.
2) Car following model is an appropriate model under free-flow traffic or heavy traffic scenarios, where **driver reaction time** is believed to be a dominant factor. Empirical studies [24] confirm that, during rush hour β' is typically a small number that represents the reaction time of a driver, following a log-normal distribution [25]. However, in light to moderate traffic, β' can be as large as 50-100 seconds and cannot be interpreted as driver reaction time. Instead, **inter-arrival time** between vehicles should be used to describe this spacing. Exponential distribution is typically assumed to describe the inter-arrival time on a single-lane road [25], even though none of the existing works, to the best of our knowledge, has technical evidence to justify this assumption.

To address both limitations, based on the above discussion, we extend the car-following model to the road-level by replacing the lane-level reaction time β' with a road-level inter-arrival time β . The lane-level car-following model in (2) can be generalized as

$$S = L_{\min} + \beta V \tag{3}$$

where β is the inter-arrival time of vehicles on any lane of the same road as observed from a fix observation point and $L_{\min}$ is the minimum spacing between any two adjacent vehicles[1]. Figure 1 shows the comparison between the lane-level headway spacing, S', and road-level inter-vehicle spacing, S, where S can be as small as 0 and as large as S'. By focusing on road-level inter-vehicle spacing S, the proposed model not only describes rush-hour heavy traffic but also captures the sparse or intermediate traffic.

However, two key parameters (the inter-arrival time β and the vehicle speed V) of extended car following model remain unclear. Rather than relying on unrealistic assumptions like many previous studies, we have conducted an empirical study from the real freeway traffic data collected by the Berkeley

[1]Both lane separation and effective vehicle length are very small (i.e., 2-3 meters), when compared to a typical transmission range (i.e., 250 m). Hence, in the remainder of this paper, we assume that $L_{\min}$ is zero.

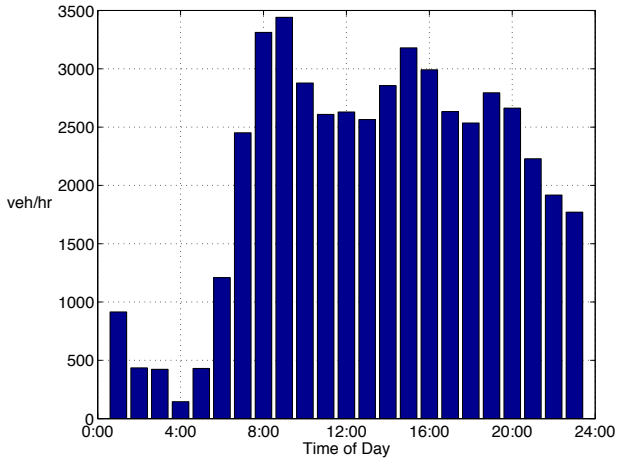

Fig. 2. Traffic volume collected from the loop detectors on I-80 on Tuesday June 27, 2006.

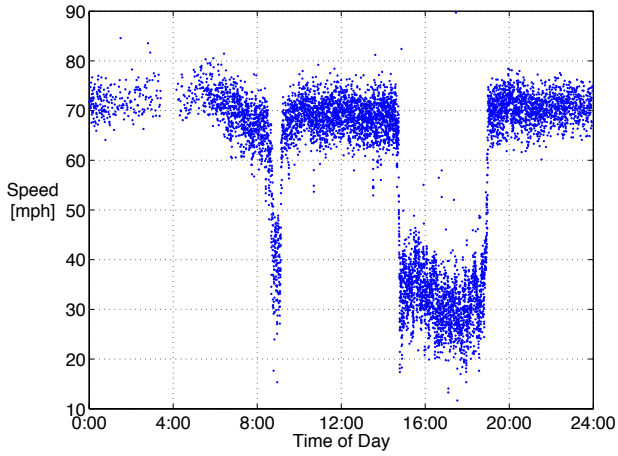

Fig. 3. Vehicles' speed extracted from the loop detectors on I-80 on Tuesday June 27, 2006.

Highway Laboratory (BHL) [26] to measure these two parameters. Incorporating empirical data into traffic model shown in Eqn. (3), we are able to investigate: (1) whether and when the network disconnection occurs; and (2) how serious this disconnected network problem could be, in real vehicle traffic situations.

IV. Road-Level Traffic Model: Empirical Study

A. Measurement of Empirical Data

To accurately calculate key parameters (β and V) of the proposed traffic model, we analyze the data collected from the dual-loop detector on the eastbound I-80 which is a 5-lane highway immediately east of San Francisco-Oakland Bay Bridge between Emeryville, CA and Berkeley, CA [26][2]. The provided traffic data were collected for 24 consecutive hours by using 1/60 second timestamps starting at midnight, June 27, 2006[3]. By measuring when vehicles enter and exit the detector loop on the road in the same direction (regardless of the lane where vehicles reside), one can extract road-level inter-arrival times β and speed of vehicles V on the freeway as observed from the location of the detector. Figures 2 and 3 show the I-80 traffic volumes and scatter plot of time-window average vehicles' speed [4] on June 27, 2006. Three different time periods with different traffic volumes and traffic flow behavior were carefully selected for our case studies, with each time period lasting for 2 hours:

1) Night traffic with very low traffic volume and high speed (1 am - 3 am);
2) Free-flow non-rush hour traffic with moderate traffic volume and high speed (10 am - 12 pm);
3) Rush-hour traffic with low speed, some intermittent congestion, and with very high traffic volume (3 pm - 5 pm).

Figure 4(a) shows the probability density function (PDF) of the inter-arrival time β on I-80 at the three selected time periods. Observe that during the night (from 1 am - 3 am), the inter-arrival time can be as long as 100 seconds while the inter-arrival times during rush hour from 3 pm - 5 pm are well below 10 seconds. Figure 4(b) shows the PDF of vehicles' speed V during three different time periods. It can be observed that, regardless of the time of day, the vehicles' speed seems to be represented by a normal distribution. In addition, the average speed is approximately 30-32 m/s during non-rush hour and is approximately 10 m/s during rush hour.

Following our proposed traffic model, for each vehicle, road-level inter-vehicle spacing S can be approximated as the product of road-level inter-arrival time between vehicles (β) and vehicles' speed (V). Intuitively, when vehicles move at slower speeds in heavy traffic conditions, drivers have more control over the vehicles and thus the safe distance is small. On the other hand, the inter-vehicle spacing is anticipated to be much longer during the low traffic volume period at night. As shown in Figure 5(a), the inter-vehicle spacing falls heavily into the distance bin of 0-20 meters during rush hour (3 pm - 5 pm); the inter-vehicle spacing during non-rush hour (10 am -12 pm) spreads over 0-350 meters; and the inter-vehicle spacing in sparse traffic during night time (1 am - 3 am) stretches to a few kilometers.

Among the three time periods, we are particularly interested in the characteristics of the network connectivity during the night time period. Normally, vehicles are viewed as being 'disconnected from one another' if they are separated by more than 250 meters (i.e., the reliable communication range of the DSRC device). One can observe from Figure 5(b) that each vehicle has only 65% chance of being able to communicate with the following vehicle during the night time period 1 am - 3 am. Note that this 35% proability of network partitioning pertains to full market penetration case, where we assume

[2]In this work, we consider 2-lane traffic behavior by extracting traffic information from the 5-lane data collected. However, our framework can also be extended to support multiple-lane traffic. We also note here that although the traffic pattern observed on I-80 may not represent traffic pattern on all highways, we believe that the proposed framework developed based on I-80 data can be applied to traffic patterns observed on other highways as well.

[3]Although the results shown in this paper pertains to the traffic data collected on one specific date, the analysis of different data sets collected on *other days* also yields similar results. This has been verified by additional data sets to the ones collected on June 27, 2006.

[4]Observe that during 3:30-4:10, there seems to be no vehicle passing by the loop detectors. This could be because of the malfunction in the hardware or software used to collect the data or maybe because there is really no traffic during that time. Since the cause of this absence is unknown, we will exclude this time period from our analysis.

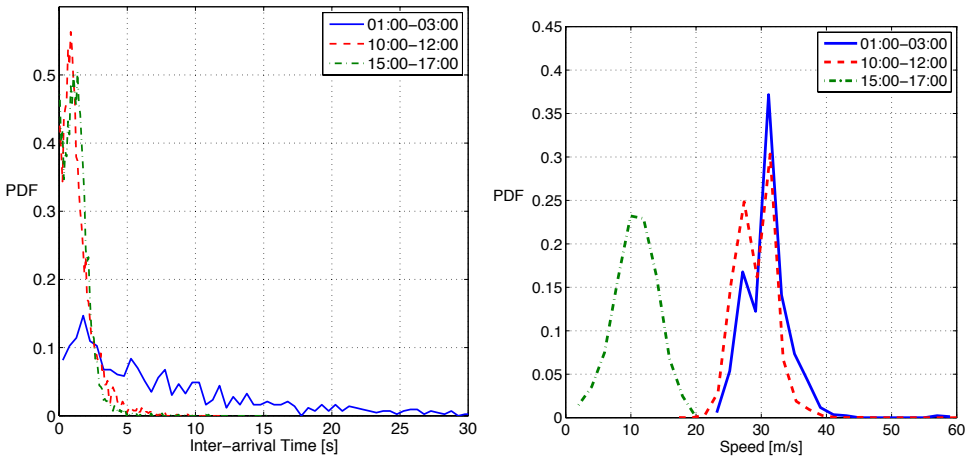

(a) PDF of inter-arrival time, β (b) PDF of vehicles' speed, V

Fig. 4. Inter-arrival time and speed statistics at three different time periods on Highway I-80, measured from empirical data.

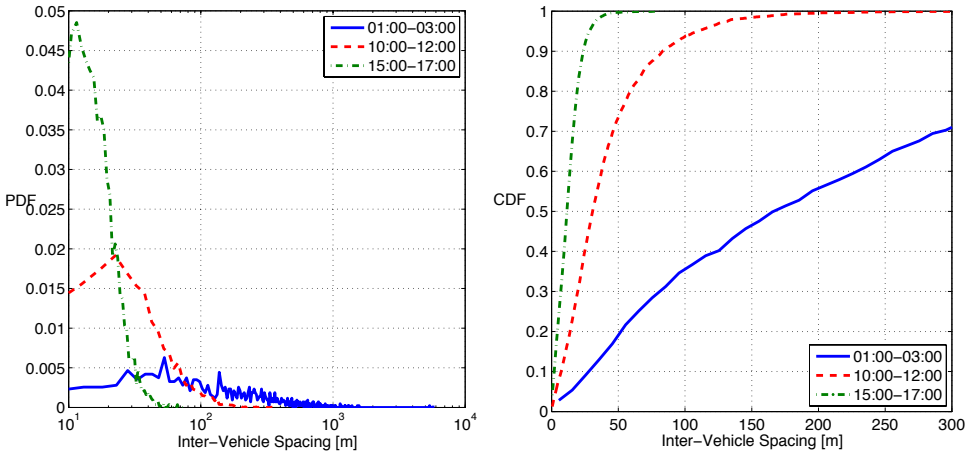

(a) PDF of Inter-vehicle spacing $f_S(s)$ (b) CDF of inter-vehicle spacing $F_S(s)$

Fig. 5. Empirical inter-vehicle spacing distribution at different time periods on Highway I-80.

that all vehicles are equipped with wireless communication capability. However, the market penetration rate during the introductory phase of the technology will be much less than 100%. Hence, as we will also show in Section IV-C, it is expected that the network disconnection will be a much more severe problem than what is presented in this section.

As a first step, in the next section, we derive the Probability Distribution Function (PDF) of inter-vehicle spacing between vehicles in a disconnected network during both light-traffic hours or during market introduction phase with low market penetration.

B. Inter-Vehicle Spacing Distribution

Based on the empirical study in Section IV, we observe that although the shape of the inter-arrival time distribution, $f_\beta(\beta)$, seems log-normal during day-time hours, the inter-arrival time of traffic after midnight to early morning seems exponential. Since we are only concerned in this paper about sparse traffic scenarios where network connectivity is low, we will assume that the inter-arrival time has an exponential distribution with parameter λ_t given by

$$f_\beta(\beta) = \lambda_t e^{-\lambda_t \beta} \tag{4}$$

where λ_t can be derived from the average traffic volume, T_v, i.e.,

$$\lambda_t \approx \frac{T_v}{3600}. \tag{5}$$

In order to test how close the exponential distribution is to the empirical distribution, we use Kolmogorov-Smirnov test (K-S test) which measures the goodness-of-fit in terms of (D_n^+, D_n^-) defined as

$$\left(D_n^+, D_n^-\right) = \max\left\{F_n(x) - F(x), F(x) - F_n(x)\right\} \tag{6}$$

where $F(x)$ is the hypothesized distribution and $F_n(x)$ is the empirical distribution. As shown in Figure 6(a), we find that the empirical inter-arrival time data can be accurately approximated by an exponential distribution during early morning hours when traffic volume is below 1000 veh/hr with D statistics of less than 3%. It can be observed from Table I that when traffic volume exceeds 1000 veh/hr, exponential distribution does not seem to be a good fit. This, however,

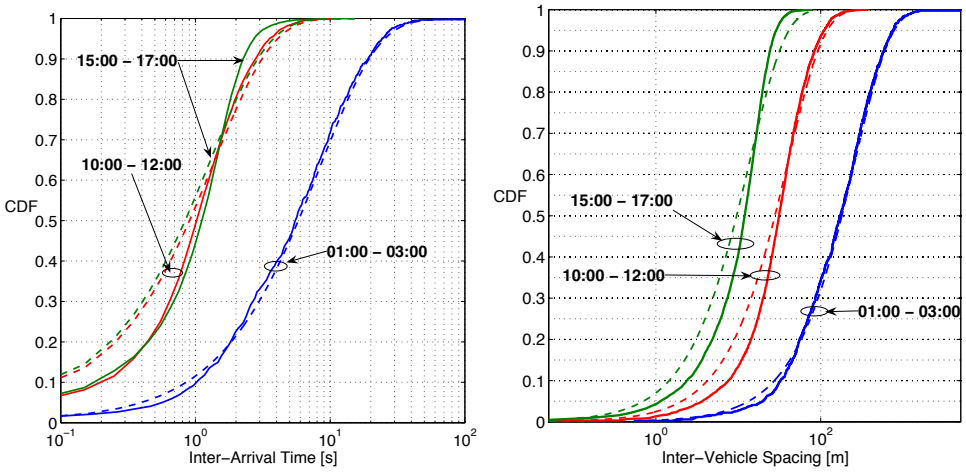

(a) CDF of Inter-arrival Time (b) CDF of Inter-vehicle Spacing

Fig. 6. Comparison of exponential distributions (dashed lines) and the empirical probability distributions (solid lines).

TABLE I
KOLMOGOROV-SMIRNOV TEST RESULTS OF INTER-ARRIVAL TIME DURING THREE DIFFERENT TIME PERIODS

Time of Day	T_v [veh/hr]	λ_t [veh/s]	(D_n^+, D_n^-) [%]
01:00 am - 03:00 am	429	0.1192	(2.89, 2.00)
10:00 am - 12:00 pm	2619	0.7276	(4.65, 4.00)
15:00 pm - 17:00 pm	2812	0.7813	(8.23, 10.98)

TABLE II
KOLMOGOROV-SMIRNOV TEST RESULTS OF INTER-VEHICLE SPACING DURING THREE DIFFERENT TIME PERIODS

Time of Day	$\overline{V}$ [m/s]	λ_t [veh/s]	λ_s [veh/m]	(D_n^+, D_n^-) [%]
01:00 am - 03:00 am	30.93	0.1192	0.0039	(2.65, 2.42)
10:00 am - 12:00 pm	29.15	0.7276	0.0250	(3.13, 9.27)
15:00 pm - 17:00 pm	10.73	0.7813	0.0728	(8.09, 9.67)

does not seem to be a major limitation as the network will be fully connected when the traffic volume exceeds 1000 veh/hr.

Similarly, the inter-vehicle spacing can also be characterized by an exponential distribution which is given by

$$f_S(s) = \lambda_s e^{-\lambda_s s} \tag{7}$$

where the parameter λ_s can be approximated as

$$\lambda_s \approx \frac{T_v}{3600 \times \overline{V}} = \frac{\lambda_t}{\overline{V}}. \tag{8}$$

As expected, the exponential distribution fits the empirical distribution well when traffic volume is below 1000 veh/hr, but it cannot be used to characterize inter-vehicle spacing when traffic volume is high. More specifically, the statistical results obtained from the K-S test show that the exponential distribution with the parameter λ_s obtained from Eqn. (8) deviates from the empirical distribution by at most 3%. However, the deviation increases to approximately 10% as traffic volume exceeds 1000 veh/hr, as shown in Table II.

Since the focus of our study is on *disconnected networks*, we are not concerned about high traffic volume cases as the vehicular network during the day seems to be fully connected with high probability, i.e., 100% during rush hour and close to 100% during day time non-rush hour (given that the vehicle's reliable transmission range is 250 m). However, these statistical results only pertain to a fully deployed network where all vehicles are equipped with a wireless communication devices. In the next section, we will investigate the impact of the market penetration rate on the distribution of the inter-vehicle spacing.

C. Impact of Market Penetration Rate on Inter-vehicle Spacing Distribution

During market introduction phase, it is expected that not every vehicle will be equipped with a wireless communication device. Clearly, low market penetration rate could exacerbate the severity of the disconnected network problem as a vehicular network could be fragmented even during rush hour with high traffic volume if the market penetration rate is too low. In this section, we will study the impact of market penetration rate on the inter-vehicle spacing distribution.

Based on the empirical inter-vehicle spacing data obtained from BHL, one can recalculate the new inter-vehicle spacing with different level of market penetration by assuming that the equipped vehicles spread out uniformly over the considered road segment. For example, the market penetration rate of 50% means that only half of the vehicles on the road are equipped with wireless communicaiton devices. Interestingly, by using the K-S test, we find that probability distribution of the spacing between equipped vehicles in a network with $x\%$ market penetration rate can also be approximated as an exponential distribution with parameter $\lambda_{sx} = x\lambda_s/100$, given by

$$f_{S_x}(s_x) = \lambda_{sx} e^{-\lambda_{sx} s_x} \tag{9}$$

and the corresponding CDF will be given as:

$$F_{S_x}(s_x) = 1 - e^{-\lambda_{sx} s_x} \tag{10}$$

Figure 7 shows a comparison between the empirical inter-vehicle spacing distributions (solid lines) and the corresponding theoretical distributions (dashed lines), for the traffic during rush hour (Figure 7(a)) and during free-flow non-rush hour

(Figure 7(b)) with 50% and 10% market penetration rate. It can be observed that as the market penetration rate decreases, the empirical distribution converges to exponential, i.e., the D statistics of the K-S test is approximately within 5% during rush hour and is within 3% during non-rush hour, for a given 10% market penetration rate. Obviously, the disconnected VANET problem caused by low market penetration is the same as the disconnected VANET problem caused by sparse network density. The traffic with certain percentage of market penetration, therefore, can be completely characterized by the same traffic model with different density.

Via a rigorous analysis of empirical highway traffic data, we find that VANETs may experience network fragmentation either due to sparse traffic density and/or because of low market penetration of wireless devices. In the next two sections, we use the empirical data presented in this section to develop deeper insights into the basic characteristics of disconnected vehicle network topology. Such a thorough understanding of disconnected vehicle network characteristic is crucial for designing a DTN (Delay Tolerant Network)-oriented routing protocol in such intermittently connected networks.

V. Characteristics of Disconnected Vehicular Ad Hoc Network: Preliminaries

Realizing that a Vehicular Ad hoc Network is prone to network fragmentation, it becomes essential to capture VANET's traffic characteristics for a better understanding of this phenomenon. Based on the empirical data, we observe that vehicles tend to move in clusters where two consecutive clusters of vehicles are normally separated by a relatively large distance.

Definition 1: *Vehicles in the same direction are said to be within the same cluster if and only if they can communicate with one another in a one-hop or multi-hop fashion. Otherwise, vehicles are said to be in different clusters. From a networking standpoint, any two adjacent vehicles belong to the same cluster if they can directly communicate with one another (i.e., within the transmission range); otherwise, these two belong to different clusters.*

According to Definition 1, the minimal separation between clusters should at least be larger than the transmission range R (i.e., 250 meters).

We show in this paper that statistical properties of clusters play an important role in disconnected VANETs. In this section, we aim to capture several key characteristics of disconnected VANETs related to clusters, including *probability of being the last vehicle in the cluster*, *average intra-cluster spacing*, *average inter-cluster spacing*, *average cluster size*, and *average cluster length*. We believe that such a study would facilitate a better understanding of the disconnected VANET problem. Later, these characteristics are also shown to be the fundamental 'building blocks' in establishing the analytical framework for analyzing network re-healing behavior, as illustrated in Section VI.

A. Probability of Being the Last Vehicle in a Cluster (P_d)

Directional broadcast transmission is favored in active safety applications for VANETs. Here, the source vehicle which detects the hazard or accident can generate a warning message and distribute to following vehicles in order to notify other drivers before they reach the potential danger on the road. However, during the directional broadcast, the warning message cannot be delivered across the cluster boundary because inter-cluster spacing is more than the transmission range R. To optimize the delay, intuitively, the last vehicle in the leading cluster is the logical choice to relay the message to other following clusters. Thus, we are interested in analyzing the probability of being the last vehicle in a cluster P_d. In other words, P_d is the probability that there are no following vehicles within the transmission range R of the last vehicle. Given the PDF of the inter-vehicle spacing in Eqn. (7), P_d is simply given by

$$\begin{aligned} P_d &= Pr\{s > R\} \\ &= 1 - F_S(R) = e^{-\lambda_s R} \end{aligned} \tag{11}$$

where $F_S(R) = 1 - e^{-\lambda_s R}$ is the Cumulative Distribution Function (CDF) of the inter-vehicle spacing. As we will show later, P_d is the metric used to calculate many other important characteristics of a disconnected VANET, such as, average cluster size, average cluster length, and average re-healing time.

B. Average Intra-cluster Spacing ($E[S_{intra}]$)

Packets travel across a cluster via a single- or multi-hop route, where the number of hops within any given cluster depends on the number of vehicles in a cluster and the spacing between two adjacent vehicles or intra-cluster spacing, S_{intra}. In this section, we are particularly interested in characterizing the intra-cluster spacing between adjacent vehicles i and $i+1$ which travel in the same cluster. Since the two vehicles belong to the same cluster, the distance between them should be less than the transmission range R. Given that the inter-vehicle spacing S has an exponential distribution, it follows that the Probability Distribution Function (PDF) of S_{intra} can be expressed as

$$f_{S_{intra}}(s_{intra}) = Pr[S|S \le R] = \frac{\lambda_s e^{-\lambda_s s_{intra}}}{1 - e^{-\lambda_s R}} \tag{12}$$

and the following lemma holds:

Lemma 1. *If the inter-vehicle spacing is exponentially distributed with parameter λ_s, then the average intra-cluster spacing is*

$$E[S_{intra}] = \frac{1}{\lambda_s} - \frac{Re^{-\lambda_s R}}{1 - e^{-\lambda_s R}}. \tag{13}$$

Proof: *Immediate from Eqn. (12).* □

C. Average Inter-cluster Spacing ($E[S_{inter}]$)

Similar to intra-cluster spacing, we are also specifically interested in analyzing the average inter-cluster spacing $E[S_{inter}]$, i.e., the expected spacing S_{inter} between the last vehicle of the leading cluster and the first vehicle of the following cluster. We believe this characteristic significantly affects the message re-healing time, as shown later, in Section VI. Obviously, in line with the concept of clusters, the distance between the last vehicle of the leading cluster and the first

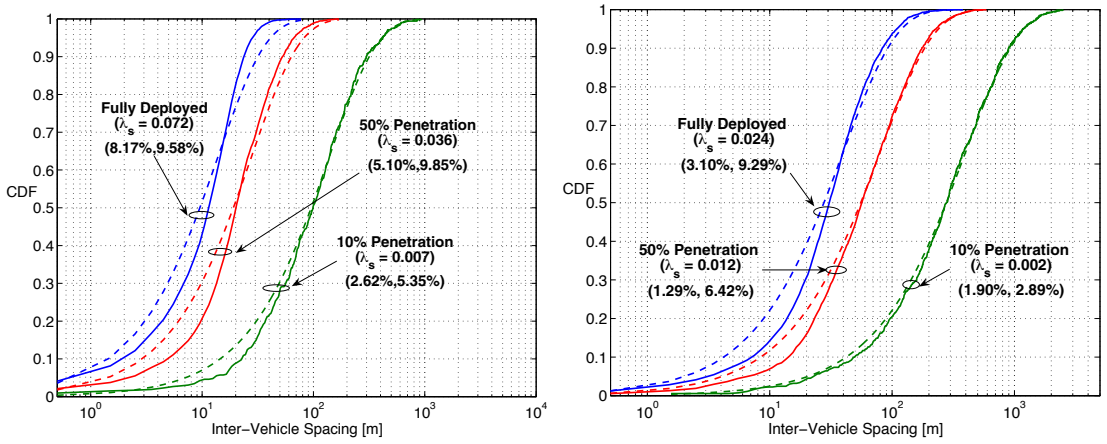

(a) Rush Hour Traffic (13 pm - 17 pm) (b) non-Rush Hour Traffic (10 am - 12 pm)

Fig. 7. Impact of market penetration rate on the empirical inter-vehicle spacing distribution (solid lines) and the hypothesized distributions (dashed lines)

vehicle of the following cluster should be larger than transmission range R. Given that the inter-arrival spacing S follows an exponential distribution, PDF of S_{inter} can be expressed as

$$f_{S_{inter}}(s_{inter}) = Pr\left[S|S > R\right] = \lambda_s e^{-\lambda_s(s_{inter}-R)}. \quad (14)$$

and the following lemma holds:

Lemma 2. *If the inter-vehicle spacing is exponentially distributed with parameter λ_s, then the expected inter-cluster spacing is given by*

$$E\left[S_{inter}\right] = R + \frac{1}{\lambda_s}. \quad (15)$$

Proof: *Immediate from Eqn. (14).* □

D. Average Cluster Size ($E[C_N]$)

Besides the intra- and inter-cluster spacing, we also study the average cluster size, i.e., the expected number of nodes within a cluster. The following lemma holds:

Lemma 3. *If the inter-vehicle spacing is exponentially distributed with parameter λ_s, then the expected number of vehicles in a cluster is*

$$E\left[C_N\right] = \frac{1}{P_d}. \quad (16)$$

Proof: *Let S_i be the inter-vehicle spacing between vehicle i and $i+1$, the Probability Mass Function (PMF) of cluster size C_N is given as*

$$\begin{aligned} f_{C_N}(1) &= \Pr\{S_1>R\} &&= P_d \\ f_{C_N}(2) &= \Pr\{S_1\le R \,\&\, S_2>R\} &&= (1-P_d)P_d \\ f_{C_N}(3) &= \Pr\{S_1\le R \,\&\, S_2\le R \,\&\, S_3>R\} &&= (1-P_d)^2 P_d. \end{aligned}$$

By induction, the PMF of cluster size C_N is

$$f_{C_N}(c_n) = P_d\left(1-P_d\right)^{c_n-1}. \quad (17)$$

Obviously, cluster size C_N follows a geometric distribution with P_d (i.e., probability of being the last vehicle in a cluster). Lemma 3 follows from Eqn. (17) and this completes the proof. □

E. Average Cluster Length ($E[C_L]$)

Alternatively, the size of a cluster can also be described by its length between the first vehicle and the last vehicle in a cluster. Hence, C_L is a function of C_N and S_{intra}. In particular, the following result holds:

Lemma 4. *If the inter-vehicle spacing is exponentially distributed with parameter λ_s, then the average cluster length is given as*

$$E\left[C_L\right] = \left(\frac{1}{P_d}-1\right)\left(\frac{1}{\lambda_s} - \frac{Re^{-\lambda_s R}}{1-e^{-\lambda_s R}}\right). \quad (18)$$

Proof: *Observe that*

$$C_L = \sum_{i=1}^{C_N-1}\left(S_{intra}\right)_i \quad (19)$$

where S_{intra} is given by Eqn.(12) and C_N has the PMF defined in Eqn. (17). Assuming that S_{intra} are i.i.d. random variables, the expected value of C_L is given by

$$\begin{aligned} E\left[C_L\right] &= E\left[E\left[C_L|C_N=k\right]\right] \\ &= E\left[E\left[\sum_{i=1}^{C_N-1}\left(S_{intra}\right)_i\right]\right] \\ &= E\left[C_N-1\right]E\left[S|S\le R\right] \end{aligned} \quad (20)$$

Using Lemma 1 and Lemma 3 in Eqn. (20) completes the proof. □

After analyzing these characteristics for a disconnected VANET in a single direction, we next study other key characteristics of a disconnected VANET comprising two directions (e.g., with traffic Eastbound and Westbound). Via such a study, we can shed light on how the disconnected network can be handled by using the opposite direction traffic for message delivery.

VI. Analysis of Disconnected Networks with Two Directional Traffic

With a conventional routing protocol, it is nearly impossible for vehicles from different clusters to communicate with one another as there is virtually no network connectivity. However, due to the deterministic topology of a VANET (road structure), passing by vehicles traveling in the opposite direction can sometimes help to restore the network connectivity at the expense of additional message delays. To give an example,

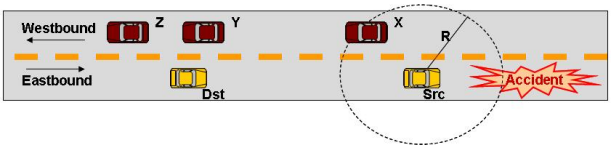

Fig. 8. Basic disconnected network scenario.

consider the scenario shown in Figure 8 where the source vehicle **Src** observes an accident and broadcasts a warning message to vehicles traveling in the same direction. Unfortunately, the target vehicle **Dst** is not within **Src**'s transmission range, R, so **Src** is disconnected from **Dst** and we have a disconnected network problem. For such a scenario, the message can still be relayed to **Dst** by using the vehicles traveling in the opposite direction as relay nodes, if **Src** is connected to either **X, Y,** or **Z**. However, it is also possible that there are no vehicles in **Src**'s range in both directions, in which case the message needs to be stored and forwarded to the appropriate relay node at a later time. In this paper, we refer to the "store-carry-forward" mechanism as *temporal relay* (or, indirect packet relay) and a normal multi-hop transmission as *spatial relay* (or, direct wireless transmission). Note that, once the **Dst** finally gets the broadcast message, it will behave like a new source and rebroadcast the message to other vehicles approaching the accident scene.

Based on the scenario described above, there are several fundamental network characteristics and performance metrics of interest; e.g., end-to-end packet delay, number of spatial and temporal relay, etc. In the following, we provide a first-order analysis of a disconnected network.

Definition 2: *For a road that has traffic moving in two opposite directions, a vehicle is said to be disconnected in the opposite direction if there are no vehicles within its transmission range in the opposite direction.*

Lemma 5. *If the inter-vehicle spacing is exponentially distributed with parameter λ_s in the message direction and λ_o in the opposite direction, then the probability of being disconnected on a two-directional road (P_{d2}), i.e., a vehicle is disconnected from both the following vehicle in the same direction and other vehicles in the opposite direction, is simply*

$$P_{d2} = e^{-(2R\lambda_o + R\lambda_s)}. \tag{21}$$

Proof: *Given an exponential inter-arrival time, vehicles' locations follow a Poisson distribution (see Section IV) and the probability of having no vehicles within the transmission range (R+R) in the opposite direction is simply given by*

$$\begin{aligned} P'_d &= \Pr[\text{no vehicles within a range of 2R}] \\ &= \frac{(2R\lambda_o)^0}{0!} e^{-2R\lambda_o} \\ &= e^{-2R\lambda_o}. \end{aligned} \tag{22}$$

The probability of being disconnected in both directions is simply the probability that there are no vehicles in the ***useful transmission range****, i.e., 2R range in the opposite direction and R in the original direction. Using Eqns. (11) and (22), we get $P_{d2} = P_d \times P'_d = e^{-(2R\lambda_o + R\lambda_s)}$.* □

In the following section, we show how P'_d and P_{d2} can be used to derive the delay incurred from temporal relay.

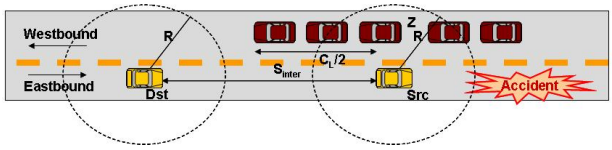

(a) Case 1.0

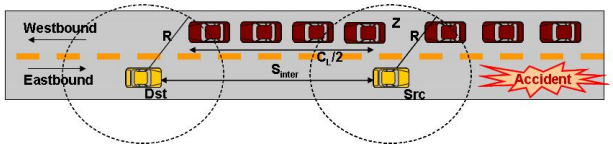

(b) Case 1.1

Fig. 9. Illustration of the scenario in case I where a packet can be spatially relayed to one of the vehicles in the opposite direction.

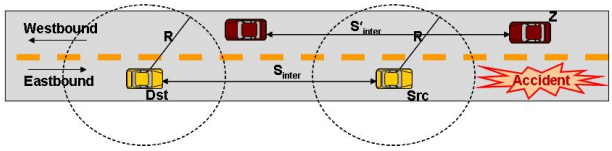

Fig. 10. Illustration of the scenario in case 2 where a packet can not immediately be relayed to vehicles in the opposite direction.

A. Re-healing time Analysis (T_r)

The *re-healing time*, T_r, is the time taken to deliver a message across two adjacent clusters, i.e., from the last vehicle in a cluster to the first vehicle in the following cluster. After receiving a packet, a vehicle can either *spatially* or *temporally* relay the packet to the following vehicle. In particular, if a vehicle is in the message's direction, a *spatial relay* is used when there is at least one following vehicle moving in the same direction or at least one vehicle moving in the opposite direction within its transmission range, and a *temporal relay* is used when the following vehicle is out of range and there is no other vehicles within its range on the road in the opposite direction. Similarly, vehicles in the opposite direction must either spatially or temporally relay the packet back to the message's original direction in the fastest possible manner. Assuming that the spatial delay is negligible, the end-to-end delay (D_{tr}) is simply the sum of all the re-healing time along the route.

In this section, we outline an approach for approximating the re-healing time based on the analytical framework presented in Section V. Consider a scenario where Src has to deliver a packet to Dst who is directly behind him but is not within his transmission range, see Figure 8. Assume that both Src and Dst are traveling eastbound with inter-arrival rate of $v_e\lambda_e$ cars/second, i.e., average vehicles' speed in the source direction is v_e and the traffic density in the source direction λ_e . Similarly, the inter-arrival rate on the westbound is assumed to be $v_w\lambda_w$ cars/second, i.e., $v_o = v_w$ and $\lambda_o = \lambda_w$, using our earlier notation. In order to relay this packet to Dst, Src could run into one of the following cases:

Case 1: Best-Case Scenario

This case occurs when Src can immediately relay his packet to Z, as shown in Figure 9.

Theorem 1. *The best-case average re-healing time is given as*

$$E\left[T_{r1}\right] = \left\{\frac{1-e^{-\lambda_e R}}{v_e+v_w}\left\{\frac{1}{\lambda_e}-\frac{1}{2}\left[\frac{1}{\lambda_w}-\frac{Re^{-\lambda_w R}}{1-e^{-\lambda_w R}}\right]\times\left[1-(k+1)(1-e^{-\lambda_w R})^k + \frac{(1-e^{-\lambda_w R})-(1-e^{-\lambda_w R})^{k+1}}{e^{-\lambda_w R}}\right]\right\} + e^{-\lambda_e R}\,\frac{R\lambda_e+1}{\lambda_e(v_e+v_w)}\right\}\times\left[1-\left(1-e^{-\lambda_w R}\right)^k\right] \quad (23)$$

where $k = \frac{2\lambda_w(1-e^{-\lambda_w R})}{\lambda_e-\lambda_e e^{-\lambda_w R}(1+R\lambda_w)}$. This occurs with probability $p_1 = 1 - e^{-2R\lambda_w}$.

Proof of Theorem 1: *See Appendix A.*

Corollary 1.1 *In a very sparse network where* $\lambda_e R \ll 1$ *and* $\lambda_w R \ll 1$*, the best-case average re-healing time is given as*

$$E\left[T_{r1}\right] \approx \frac{1}{v_e+v_w}\left[\frac{1}{\lambda_e}+R\right]. \quad (24)$$

Proof of Corollary 1.1: *See Appendix A.*

Corollary 1.1 suggests that the average re-healing time in the best-case scenario depends only on the traffic density of the message-forwarding direction, i.e., on λ_e. In addition, it also indicates that as the traffic density becomes very sparse (i.e., as $\lambda_e \to 0$), then the average re-healing time becomes very large (i.e., $E\left[T_{r1}\right] \to \infty$).

Case 2: Worst-Case Scenario

In the worst-case, Src cannot immediately relay his packet to Z who is moving Westbound, as shown in Figure 10. Hence, Src has to store and carry the packet until Z comes into his range.

Theorem 2. *The worst-case average re-healing time is given as*

$$E[T_{r2}] = \frac{1-(1-e^{-\lambda_e R})^M-e^{-\lambda_e R}}{(1-e^{-\lambda_e R})(v_e+v_w)}\times\left\{\left(\frac{1}{e^{-\lambda_e R}}-1\right)\left(\frac{1}{\lambda_e}-\frac{Re^{-\lambda_e R}}{1-e^{-\lambda_e R}}\right)-\frac{1}{2\lambda_w}\right\} + \frac{1}{2\lambda_w(v_e+v_w)}+\frac{R\lambda_e+1}{\lambda_e(v_e+v_w)} \quad (25)$$

where $M = \left\lfloor \frac{\left(1-e^{-\lambda_e R}\right)\left(\frac{\lambda_e}{\lambda_w}-R\lambda_e\right)}{1-e^{-\lambda_e R}-Re^{-\lambda_e R}} \right\rfloor$. *This occurs with probability* $p_2 = e^{-2R\lambda_w}$.

Proof of Theorem 2: *See Appendix B.*

Corollary 2.1 *In a very sparse network where* $\lambda_e R \ll 1$ *and* $\lambda_w R \ll 1$*, the worst-case average re-healing time is given as*

$$E\left[T_{r2}\right] \approx \frac{1}{v_e+v_w}\left[\frac{1}{2\lambda_w}+\frac{1}{\lambda_e}+R\right]. \quad (26)$$

Proof of Corollary 2.1: *See Appendix B.*

Observe that if the Src runs into the worst-case scenario, the average re-healing time depends on the density of the traffic in both directions since the Src will also have to buffer the message until it can find a vehicle in the opposite direction who can carry the message. Corollary 2.1 suggests that the average re-healing time $\to \infty$ as $\lambda_w, \lambda_e \to 0$. In addition, Corollary 2.1 also indicates that in the limit, the message holding time for a source is $\frac{0.5}{\lambda_w(v_w+v_e)}$ and the message relay time is $\frac{1/\lambda_e+R}{(v_w+v_e)}$.

Theorem 3. *Given that Src is disconnected from Dst, the expected per-gap re-healing time* T_r *can be approximated by the following expression:*

$$E\left[T_r\right] = \left(1-e^{-\lambda_w 2R}\right)\times E[T_{r_1}] + e^{-\lambda_w 2R}\times E\left[T_{r_2}\right] \quad (27)$$

where $E[T_{r_1}]$ *and* $E[T_{r_2}]$ *are given by Theorems 1 and 2 (Eqns. (23) and (25)).*

Proof of Theorem 3: *See Appendix C.*

Corollary 3.1 *In a very sparse network where* $\lambda_e R \ll 1$ *and* $\lambda_w R \ll 1$*, the average re-healing time is given as*

$$E\left[T_r\right] \approx \frac{1}{v_e+v_w}\left[\frac{1}{2\lambda_w}+\frac{1}{\lambda_e}\right]. \quad (28)$$

Proof of Corollary 3.1: *See Appendix C.*

Observe that in the limiting case where λ_e and λ_w are very small, the average re-healing time given in Corollary 3.1 is only slightly less than the average worst-case re-healing time given in Corollary 2.1. This implies that the Src runs into the worst-case scenario with high probability in a very sparse network.

We will show in the next section, that the analytical framework developed in this section (and especially Eqn.(27) given above) is a very good approximation to the actual re-healing time of a disconnected VANET. As a sanity check, in the extreme scenario where there is very low network connectivity (i.e., both λ_e and λ_w are very small or close to 0), by using our analytical results presented in this section, it can easily be shown that the best-case probability (or p_1) can be approximated as 0, while the worst-case event occurs with probability p_2 = 1. Thus, the worst-case re-healing time becomes, as expected, ∞. This is because in such a scenario, it takes an infinite amount of time to encounter another vehicle on the road. As for the other extreme scenario where λ_e and λ_w are non-zero and the transmission range $R \to \infty$, then the probability of having a disconnected network or P_d shown in Eqn. (11) becomes 0 which implies that the network is well-connected.

In the following section, we resort to a simulation study to further analyze how other network parameters, e.g., speed and network density, affect disconnected networks.

VII. Disconnected Networks: Simulation Study

In this section, via extensive Monte Carlo simulations, we not only validate our analytical results obtained in Sections V and VI, but also shed light on how the *store-carry-forward* mechanism works in disconnected VANETs, so that we are able to examine the feasibility of this technical approach.

A. Simulation Model

In the following, we outline the VANET topology, mobility model, and data traffic model assumed in the customized event-driven Monte-Carlo simulator developed by the authors.

- *Network Topology:* we assume a straight freeway segment of two-lane highway going in two opposite directions, where the distribution of the inter-vehicle spacing is given by Eqn. (7). Thus, the overall number of vehicles in the considered segment can implicitly be determined by the corresponding value of λ_s parameter.
- *Mobility Pattern:* All vehicles within the network are assumed to travel at a constant speed and maintain the same spacing from the leading vehicle until it exits the network, so that there is no passing or lane changing. In addition, the last vehicles in any given cluster will remain

disconnected from the first vehicle in the succeeding cluster until they exit the network. Furthermore, we also use an open system model where vehicles who exit the network do not re-enter back into the network. Instead, new vehicles are generated and get reinserted into the network according to the assumed inter-arrival time distribution.

- *Data Traffic Model:* In order to avoid any bottleneck or buffering issue, we assume that there is at most 1 packet in the network at all times. To eliminate pathological situations, we also assume that a new packet gets generated after the destination vehicle exits the network. Using this packet generation model, we can ensure that the network topology seen by packet j is different from that seen by packet $j+1$. To be specific, in our simulation, packet generation rate is assumed to be 0.01 packets/min, i.e., one broadcast at every 100 minutes, so that the topologies seen by any two consecutive packets are completely different.
- *Network Communication Model:* The transmission range is set as 250 m in our simulation, which follows the FCC regulations. Source and destination vehicles are selected randomly from the traffic on the westbound road. Here, the only criteria is to pick the ones that are approximately X km apart. In terms of detailed protocol operations, we assume that any packets arriving at a well-connected node on the eastbound road get re-forwarded immediately according to the shortest-path routing algorithm, while any packets arriving at the last vehicle in the cluster (i.e., the network disconnection situation occurs) need to be stored. Later, the stored packets will be forwarded to the first westbound vehicle encountered when appropriate. Vehicles traveling westbound thus help store-carry-forward the packet if the network on the eastbound is disconnected.

  Since we are only interested in a network with very low connectivity and low data traffic load, we argue that MAC and PHY layers have very little impact on the overall network performance. Hence, in this work, we assume ideal MAC/PHY layers where a packet arriving at network layer gets transmitted right away without any contention at the MAC layer and all the transmitted packets arrive at the intended destination without error. Under this assumption, the delay incurred at the MAC/PHY layers will be much smaller than the delay incurred from the temporal relay which is typically on the order of seconds. Therefore, we will also assume that the spatial delay due to direct wireless transmission is zero.

In our simulations, we vary λ_s, v_e, and v_w parameters to investigate their impact on various characteristics of disconnected VANETs, especially those related to network re-healing behavior. Since we are not interested in what happens when the network is fully connected, the results presented in this section are averaged over the cases where there is at least one network disconnection on the eastbound road during a packet transmission. Each simulation point is an average of 10,000 such cases.

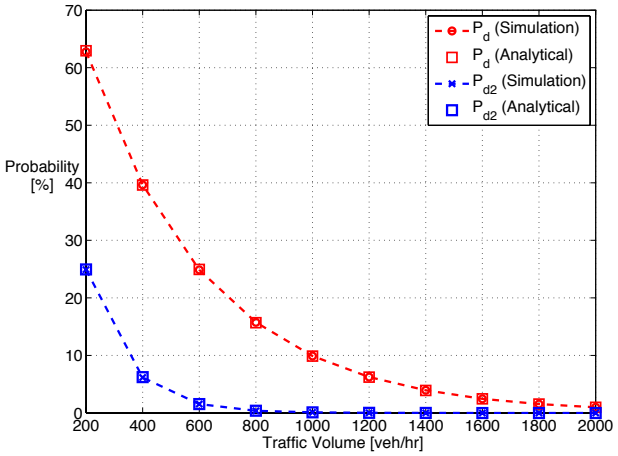

Fig. 11. Probability of being disconnected on a one-directional and two-directional roads.

B. Validation of Characteristics of Disconnected Vehicular Ad hoc Network

In this section, we conduct Monte-Carlo simulations according to the model described in Section VII-A. Such a study not only validates the analytical framework presented in Section V, but also helps us gain more insight into the basic characteristics of disconnected VANETs.

For this section, we consider VANET topologies on a 50 km road section. Also, the source is approximately 10 km away from the destination, where all vehicles are assumed to travel at a constant speed of 30 m/s. Vehicles enter into the network according to a Poisson distribution with λ_t ranging from 0.05 to 0.55 veh/s, i.e., traffic volume ranging from approximately 200 to 2000 veh/hr. In this subsection, we mainly vary the traffic volume to evaluate how it impacts various characteristics of disconnected networks.

Figure 11 shows the probability of being disconnected on both networks composed of one-directional vehicle traffic and network composed of two-directional vehicle traffic, at various network densities. Not only does our analytical result in Section V-A matches the simulation results, it also matches the empirical results presented in Section IV-A. For example, the empirical study shows that the probability of being disconnected is approximately 35% during late night hours when the observed traffic volume is 429 veh/hr: both our anlytical and simulation results also suggest the same probability. As expected, the lower the traffic volume, the higher the probability of being disconnected in one or both directions. However, the probability of being disconnected in a network composed of vehicle traffic in two directions is much smaller than its counterpart that consists of traffic in only one direction. These results suggest that a routing protocol can greatly benefit from using opposite traffic to populate the network and increase the network connectivity.

Figure 12 shows the simulation and analytical results for intra- and inter-vehicle spacing, and average cluster size (in terms of number of vehicles) and the cluster length. Again we observe an excellent match between the predictions of our analytical framework and the simulation results. As expected, as the traffic volume increases, the average inter-vehicle spacing

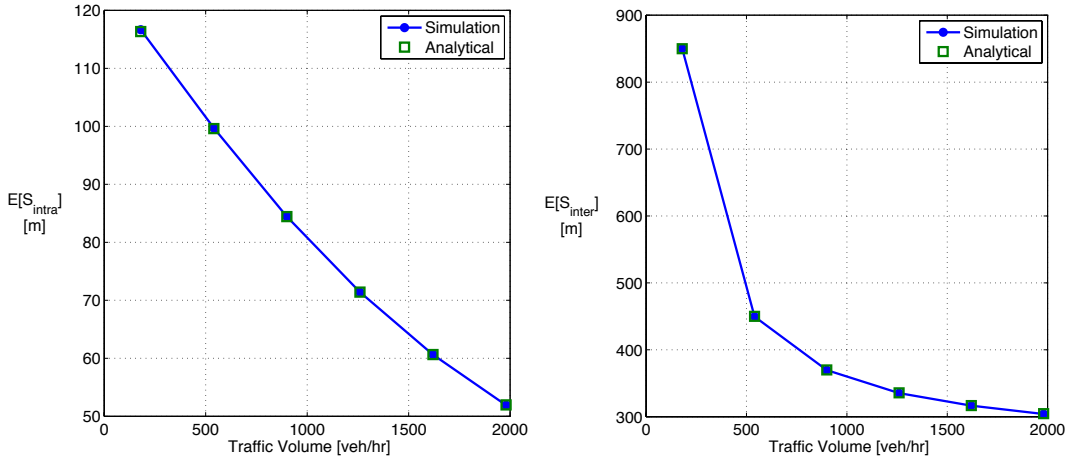

(a) Average intra-cluster spacing

(b) Average inter-cluster spacing

(c) Average number of vehicles in a cluster

(d) Average cluster lengths

Fig. 12. Inter-vehicle spacing and cluster size statistics.

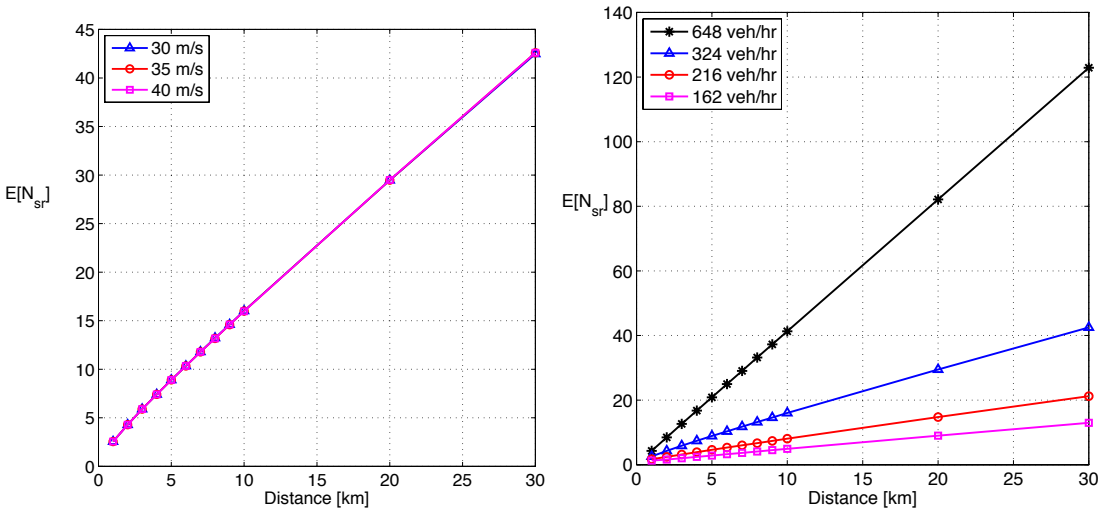

(a) Impact of vehicles' speed

(b) Impact of network density

Fig. 13. Average spatial hop count to a node that is X km away.

gets smaller; hence, E[S_{inter}] and E[S_{intra}] also get smaller. Since the probability of being disconnected also gets smaller as traffic volume increases, in turn, the average cluster size and cluster length increases. As we have shown in Section VI-A, these statistics can be used to calculate certain routing performance such as re-healing time. These results can also

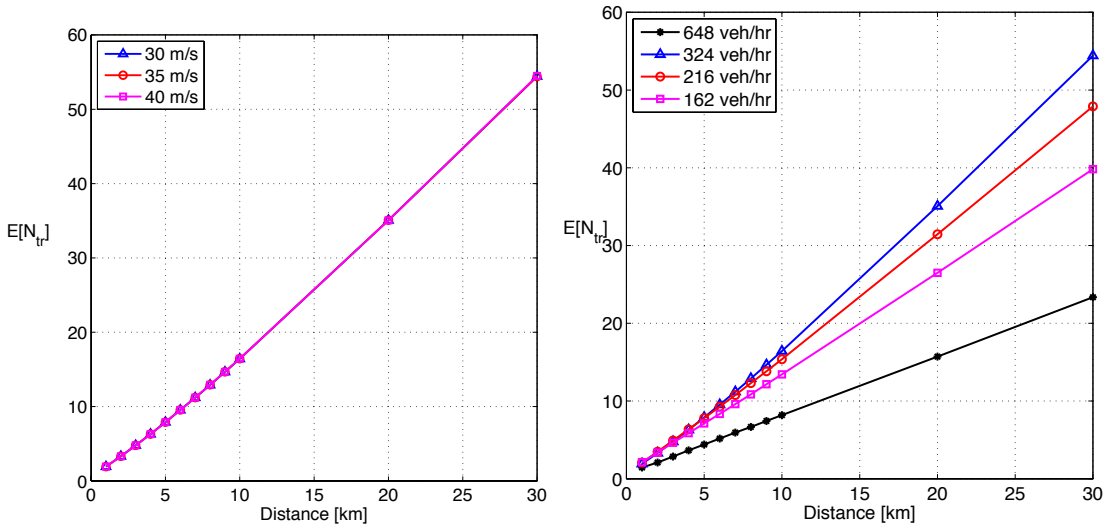

(a) Impact of vehicles' speed (b) Impact of network density

Fig. 14. Average temporal hop count to a node that is X km away.

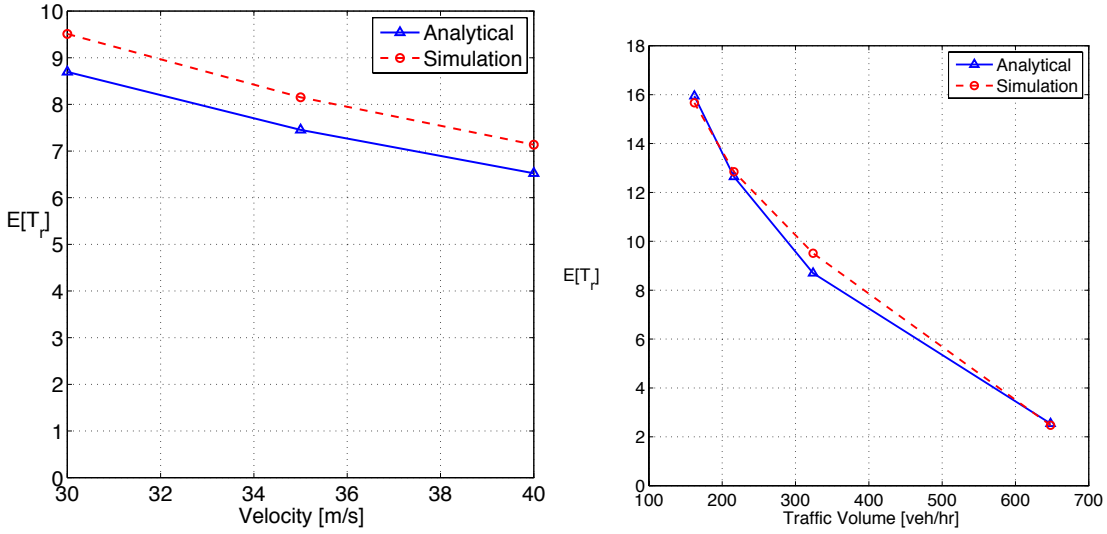

(a) Impact of vehicles' speed (b) Impact of network density

Fig. 15. Average per-gap temporal delay: Simulation results (dashed lines) and analytical results(solid lines).

be used to predict other parameters such as the spatial and temporal hop counts, etc. For example, given the distance between source and destination and the average cluster size in terms of E$[C_N]$ and E$[C_L]$, one can roughly estimate how many times a packet needs to be relayed temporally and spatially. Clearly, the larger the cluster length, the higher the spatial hop count and the lower the temporal hop count.

C. Routing Performance in Disconnected Networks

In this section, we study disconnected VANETs from a networking standpoint and consider their routing performance in terms of the total end-to-end delay, the spatial and temporal hop counts, and the per-gap re-healing time. To the applications, the total end-to-end delay, which is the time taken to deliver the message to the destination, is an important metric which can be used to determine whether the proposed routing mechanism can deliver acceptable performance or not. Other metrics, however, serve as intermediate parameters which can help to explain how the routing mechanism works in disconnected VANETs in detail. For example, the per-gap re-healing time, which is the duration of time the packet needs to be stored at the relay node, is another important metric that allows us to get a better understanding of how a routing protocol should be designed so that it provides enough buffer space for holding the routing messages. In addition, the spatial and temporal hop counts are factors which contribute to the overall end-to-end delay.

In addition to the simulation model described in Section VII-A, we assume that the distance between source and destination varies from 1 km to 30 km. According to the analytical framework presented in Section VI, one can immediately observe that routing delay depends on transmission range, vehicles' speed, and, most importantly, network density and market penetration rate. Since transmission power is

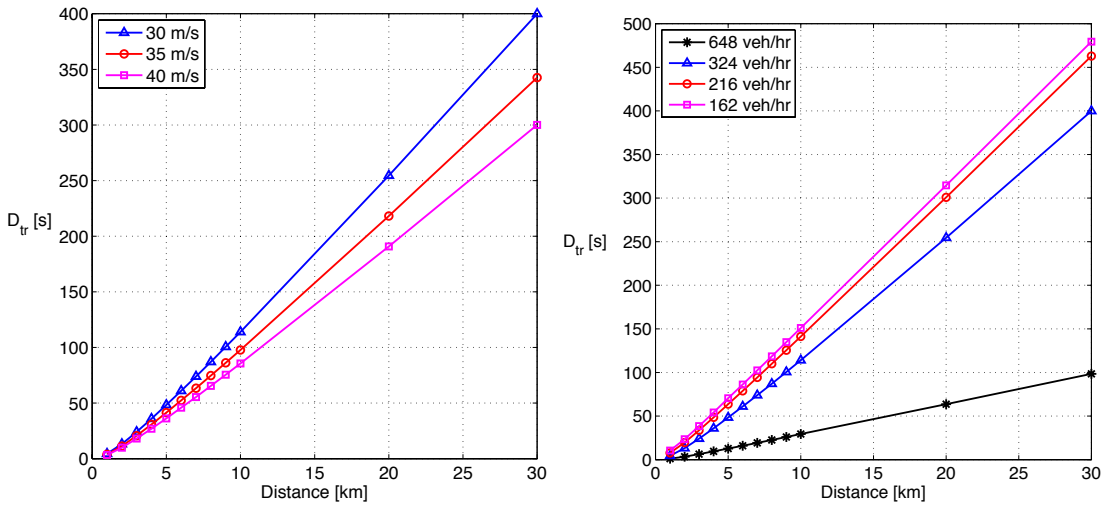

(a) Impact of vehicles' speed (b) Impact of network density

Fig. 16. Average total end-to-end delay required to transmit a packet to a node that is X km away.

controlled by regulation and the impact of market penetration can be completely characterized by various traffic densities, we will focus only on the impact of vehicles' speed and network density in the remainder of this paper.

1) Impact of Vehicles' Speed: To study the impact of vehicles' speed, we fix the network density by assuming λ_s = 0.003 (which matches the empirical late night traffic).

Figures 13(a) and 14(a) show the average spatial hop count E[N_{sr}] and temporal hop count E[N_{tr}] to a destination node, which is 1 km to 30 km away from the source. Observe that, because the network connectivity is roughly the same in all three velocity cases, when the average inter-vehicle spacing is fixed to the same value, the values of E[N_{sr}] and E[N_{tr}] in each case are approximately the same. Considering the fact that E[N_{sr}] and E[N_{tr}] are the same and the observation that the per-gap re-healing time is shorter in a highly mobile network, as shown in Figure 15(a), the total delay D_{tr} is longer in the low-mobility scenario, as shown in Figure 16(a).

Although these end-to-end delay results may seem too long for normal multi-hop applications (i.e., on the order of several minutes), they are within acceptable range for some VANET applications. For example, Figure 16(a) shows that it takes about 2 minutes for a packet to arrive at a destination vehicle 10 km away from the source. Consider a scenario where a road-side-unit (RSU) broadcasts a message which directs drivers to take an alternative route, the driver who is 10 km away from the RSU at the time of the broadcast would still be notified well ahead of time to make a rerouting decision (i.e., he will be about 6.4 km away from the RSU by the time he receives the message). Note that if a network is fully connected, the end-to-end delay should be well below 1 second.

2) Impact of Network Density: Similarly, one can also investigate the impact of network density (and the impact of market penetration) by fixing the average vehicle speed and vary λ_s, according to the level of the traffic volume or the level of market penetration of interest. Intuitively, as the network gets sparser or as the traffic volume or market penetration rate decreases, the temporal hop count should increase while the spatial hop count should decrease. To the contrary, as shown in Figure 13(b) and 14(b), the results show that the temporal hop count decreases when the traffic volume drops below 300 veh/hr. This is due to the fact that the average per-gap re-healing time is much longer in the scenario with low effective traffic volume (volume of vehicles with wireless devices): there are fewer but larger gaps in the sparse network. As shown in Figure 15(b), the expected per-gap re-healing time is almost doubled when traffic volume drops from 300 veh/hr to 150 veh/hr. As a result, the end-to-end delay is longer in the case with low effective traffic volume although the temporal hop count is much smaller than in the dense network scenario, as seen in Figure 16(b).

Although, low effective network density exacerbates the disconnected network problem, on average, drivers will still be informed well ahead of time prior to reaching the RSU or accident scene. For example, in the worst case scenario with 162 veh/sec, a vehicle that is 10 km away from the RSU at the time of the original broadcast will receive the message 2.5 mins later when he will be at approximately 5.5 km away from the RSU.

In addition to the simulation results presented, Figure 15 also show that the analytical framework we developed (see Eqn. (27)) gives a good approximation for the actual per-gap re-healing time obtained from the simulation.

D. Microscopic Analysis of Per-Gap Re-healing Time

In order to gain more insight into the disconnected network problem, it is crucial to understand how the message gets relayed to the final destination, how long the disconnected vehicle takes to discover relay vehicles, and how fast the relay vehicles can get the message to the destination vehicle. Figure 17 presents the results of such a microscopic analysis towards the details of disconnected network and its re-healing behavior. Also, Figure 17 shows the impact of vehicles' speed and network density on the three cases previously described in Section VI-A.

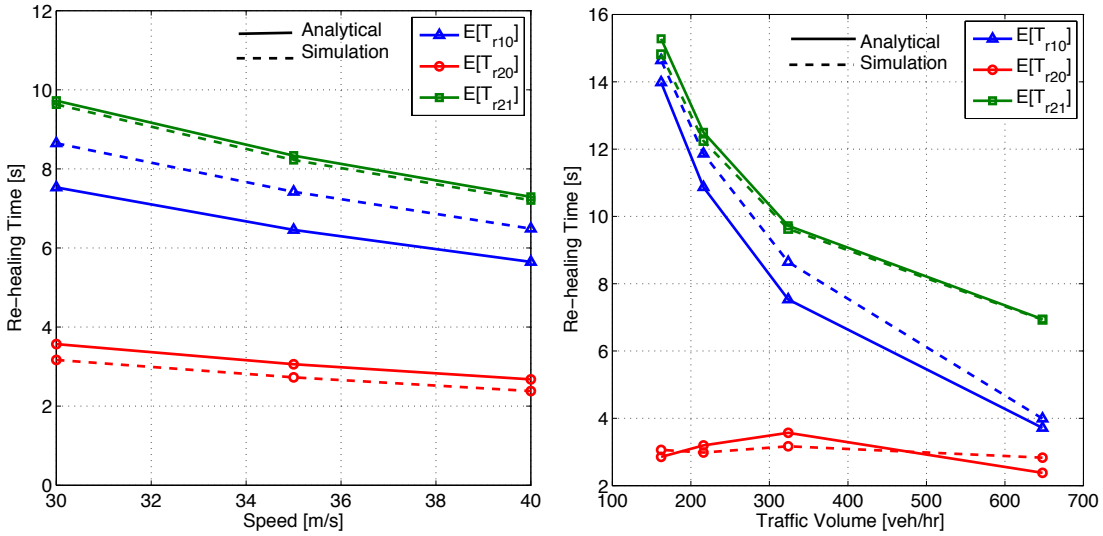

(a) Impact of vehicles' speed

(b) Impact of network density

Fig. 17. Average temporal delay of the three different scenario previously described in Section VI-A: Simulation results (dashed lines) and analytical results(solid lines).

As shown in Figure 17(b), the network density seems to significantly impact the detailed behavior of disconnected network re-healing performance. During a traffic intensity of 650 veh/hr: (1) it only takes, on average, 2-3 seconds for a disconnected vehicle in the message's direction to discover a relay node in the opposite direction regardless of the traffic volume, as shown in the E[T_{r20}] curve; (2) Vehicle in the opposite traffic has to buffer the packet for only about 4 seconds on average if a disconnected vehicle in the original direction is connected to vehicles in the opposite direction, as shown in the E[T_{r10}] curve; (3) If the disconnected vehicle cannot find a relay node right away, the packet needs to be buffered by one of the vehicles in the opposite direction traffic for a slightly longer duration, i.e., 7-15 seconds, as shown in the E[T_{r21}] curve. In addition, relay vehicles in the opposite direction will have to buffer the message for a longer time as traffic volume decreases (as shown in E[T_{r10}] and E[T_{r21}] curves).

We find that vehicle speed also impacts the re-healing behavior of a disconnected network, as shown in Figure 17(a). This observation further validates our observation in Figure 15. As the vehicle speed increases, the delay in all three cases decreases.

The (per-gap) re-healing time results are useful tools, when one designs routing protocols and determine which applications can function in such a disconnected network. For example,

1) A routing protocol can use the average re-healing time to determine the minimum buffer space it needs for storing a packet or determine the hello packet broadcast frequency, so that the relay node can be found as quickly as possible without adding too much overhead traffic into the network.
2) The VANET applications may also need to acknowledge the network disconnection by adjusting the traffic load. Correct prediction of per-gap re-healing time can help to evaluate whether the data traffic overload the underlying disconnected VANET.

VIII. Conclusions & Future Work

We have developed a comprehensive approach for studying the severity of the disconnected network phenomenon in routing messages in Vehicular Ad Hoc Networks. The proposed approach uses statistical models extracted from measured data on I-80 freeway in California. Using these statistical models, we have developed an analytical framework that sheds light on the major characteristics of disconnected VANETs. The results of the extensive Monte-Carlo simulations conducted verify the validity of our comprehensive analytical framework and show that our analytical framework provides good estimates to key performance metrics such as the average re-healing time. In particular, our results show that while the average re-healing time will be on the order of several seconds to a few minutes on I-80 type of freeways, this may still be troublesome for conventional ad hoc routing protocols such as AODV and DSR. Thus, the disconnected network problem appears to be an important issue to resolve in emerging VANET applications. Moreover, our simulation results verify that the store-carry-forward mechanism provides a potential solution to routing in disconnected networks.

As part of our future studies, one of our immediate goals is to develop routing protocols that can seamlessly handle the two extreme cases: well-connected networks and disconnected networks. The former leads to the "broadcast storm" problem while the latter makes routing (even for safety applications) a major challenge. For example, the broadcast agent should use one of the back-off mechanisms proposed in [2] to cope with broadcast storm on a per-hop basis. However, in order to cope with the disconnected scenario, each vehicle that broadcasts or rebroadcasts should buffer the message until it overhears the rebroadcast of the same message from other vehicles. After a certain period of time, if the vehicle still does not receive any

new broadcast, it should continue to periodically broadcast until the message reaches at least one new vehicle or until the message lifetime expires. Ongoing work is focused on designing new VANET routing protocols that can handle at least 3 different cases: normal traffic, dense traffic, and sparse traffic [27].

ACKNOWLEDGMENTS

The authors would like to thank Dr. Chaminda Basnayake (General Motors, MI), Samuel Yang, Saneesh Apte, and J. D. Margulici (California Center for Innovative Transportation, UC Berkeley) for providing us with invaluable traffic data. Prof. Ozan Tonguz would like to thank General Motors Corporation for sponsoring this research project at Carnegie Mellon University.

APPENDICES

APPENDIX A: *Proof of Theorem 1*

Best-Case scenario

As illustrated in Figure 9, Src can immediately relay his packet to Z spatially who is moving Westbound. It is important to understand that Proof of Theorem 1 (as well as the proofs of Theorems 2 and 3) will use the steady-state scenarios encountered in broadcasting a message (as opposed to transient scenarios) to the Region of Interest (ROI) on a typical highway. Once a packet arrives at Z, there can be two possible sub-cases which leads to the Proof of Theorem 1:

- **Case 1.0:** None of the vehicles in Z's cluster can communicate with Dst. Assume that the lane separation length is negligible and Src is located in the middle of Z's cluster (statistically speaking, this is a reasonable assumption), then case 1.0 happens if half of the Z's cluster length is less than $S_{inter} - R$ and the probability of case 1.0 is given by

$$p_{10} = \Pr\left[\frac{C_L}{2} \leq S_{inter} - R\right] \tag{A.1}$$

where C_L is the cluster length and $S_{intra} - R$ is the distance from Z to Dst's transmission zone. In order to get a closed-form expression, we assume that vehicle spacing within Z's cluster is E[S_{intra}] and that the average inter-cluster distance from Src to Dst is E[S_{inter}]. Hence,

$$\begin{aligned} p_{10} &\approx \Pr\left[\frac{C_N \times E\left[S_{intra}\right]}{2} \leq E\left[S_{inter}\right] - R\right] \\ &\approx \Pr\left[C_N \leq \frac{2\left(E\left[S_{inter}\right] - R\right)}{E\left[S_{intra}\right]}\right] \\ &\approx \Pr\left[C_N \leq k\right] \\ &\approx 1 - \left(1 - e^{-\lambda_w R}\right)^k \end{aligned} \tag{A.2}$$

where $k = \frac{2\lambda_w(1-e^{-\lambda_w R})}{\lambda_e - \lambda_e e^{-\lambda_w R}(1+R\lambda_w)}$. Similarly, given that $\frac{C_L}{2} \leq S_{inter} - R$, the conditional expected re-healing time $E\left[\mathrm{T}^0_{r_{10}}\right]$ incurred from this case is simply the time the first vehicle in the cluster takes to come into contact with Dst, which can be expressed as

$$\begin{aligned} E\left[\mathrm{T}^0_{r_{10}}\right] &\approx \frac{E[S_{inter}] - R - E\left[\frac{C_L}{2} \middle| \frac{C_L}{2} \leq S_{inter} - R\right]}{v_e + v_w} \\ &\approx \frac{\frac{1}{\lambda_e} - \frac{E[S_{intra}]}{2} E[C_N | C_N \leq k]}{v_e + v_w} \end{aligned} \tag{A.3}$$

where

$$\begin{aligned} E[C_N | C_N \leq k] &= 1 - (k+1)\left[F_{S_w}(R)\right]^k \\ &\quad + \frac{F_{S_w}(R) - \left[F_{S_w}(R)\right]^{k+1}}{1 - F_{S_w}(R)} \end{aligned} \tag{A.4}$$

and S_w is the inter-vehicle spacing on the Westbound road.

At this point, we make the observation that Case 1.0 could involve two different subcases: i) Src belongs to a cluster of size larger than 1 (i.e., $C_N > 1$); ii) Src is in a cluster of size 1 (i.e., C_N = 1). While (A.3) covers case i), we need to consider case ii) as well. If there is, on average, only one vehicle in a cluster (i.e., no clusters), it can be shown that the conditional expected re-healing time is given by

$$\begin{aligned} E\left[T^1_{r_{10}}\right] &\approx \frac{R + E\left[S_{inter}\right] - R}{v_e + v_w} \\ &\approx \frac{R\lambda_e + 1}{\lambda_e\left(v_e + v_w\right)}. \end{aligned} \tag{A.5}$$

For example, once Z relays the packet back to Dst spatially, Dst will have to immediately relay the packet back to Z spatially if Dst and Z are the only vehicles in the clusters. Hence, Z will be at least R + E[S_{inter}] away from the succeeding cluster. This case occurs with probability P_d. Hence, the expected re-healing time for case 1.0 can be computed as

$$E\left[T_{r_{10}}\right] = (1 - P_d) \times E\left[T^0_{r_{10}}\right] + P_d \times E\left[T^1_{r_{10}}\right]. \tag{A.6}$$

- **Case 1.1:** One of the vehicles in Z's cluster can relay a packet back to Dst so Src is spatially connected to Dst. The probability of this event happening is simply the complement of p_{10} and is given by $p_{11} = 1 - p_{10}$ and the average re-healing time is

$$E\left[T_{r_{11}}\right] \approx 0. \tag{A.7}$$

Now, the best-case average re-healing time can be computed as:

$$E\left[T_{r_1}\right] = E\left[T_{r_{10}}\right] p_{10} + E\left[T_{r_{11}}\right] p_{11}. \tag{A.8}$$

Since we assume that spatial delay is negligible, Theorem 1 follows from (A.6), (A.7), and (A.8) by using (11), (A.2) - (A.5), and Lemmas 1 and 2. □

Proof of Corollary 1.1

Follows from Theorem 1, by assuming that $\lambda_e R \ll 1$, $\lambda_w R \ll 1$, and by using a first-order Taylor series approximation on the RHS of Eqn. (23) where $e^{-\lambda_e R} \approx 1 - \lambda_e R$ and $e^{-\lambda_w R} \approx 1 - \lambda_w R$. □

APPENDIX B: *Proof of Theorem 2*

Worst-case scenario

Worst-case scenario occurs when Src cannot immediately relay the message to Dst. The re-healing time for this case is simply the summation of the following two delay components:

i) the time until Src comes into contact with the car that can relay the message back to the original direction, i.e., vehicle Z;

ii) the time that the relay vehicle Z has to carry the message until it comes into Dst's transmission range.

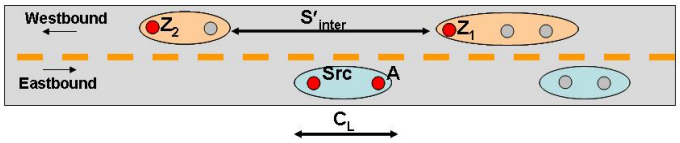

(a) Small cluster

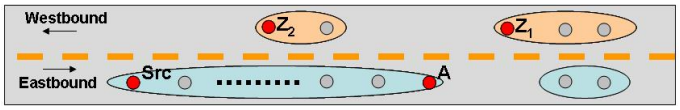

(b) Large cluster

Fig. 18. Illustration of two possible worst-case scenarios in the steady-state. The new source (Src) could be a member of either a large or a small cluster.

Again, just like Appendix A, here we also use the steady-state scenarios as the basis of our subsequent derivations. Consider Figure 10 for the worst-case again. In the worst-case scenario, the source is disconnected from the destination in its own lane as well as the opposite lane. To simplify things, assume that the source is the only car in its own cluster (this assumption does not always hold but it is valuable for understanding certain key concepts). How much more time will be needed to come into the transmission range of the next car in the opposite lane? A moment's reflection reveals that the next car's distance to the original source will be (using the well-known memoryless property of exponential distribution) $1/2\lambda_w$. This implies that in the worst case scenario, the next car approaching the source from the opposite lane is, on average, $1/2\lambda_w$ meters away. Of course, in a typical scenario, the source might have additional cars in its own cluster following it, in which case, the last vehicle in the cluster will be in charge of store-carry-forward the message.

In addition to this key observation, we also observe that when one considers the dissemination of the broadcast message from the original source, one can encounter two very different situations:

a) The new source and destination could be members of a small cluster whereby the last member of this cluster will be disconnected in both directions in which case the last car in this cluster becomes the new source (or the car that stores the message) till it finds a new car in the opposite lane to relay the message.
b) The new source (as opposed to the original broadcasting source) and destination might be members of a large cluster in the lane of interest (where accident happens) such that the last car in that cluster does not know where the closest relay vehicle is.

Figure 18 depicts these scenarios.

(i) **Temporal delay from Src to Z**:

i.1) Src is a member of a small cluster whose length is less than E[S'_{inter}] $-2R$ and is not in the same cluster as the original sender. Hence, there can be at most M vehicles in the cluster, where M is given by

$$M = \left\lfloor \frac{E\left[S'_{inter}\right] - 2R}{E\left[S_{intra}\right]} \right\rfloor \tag{B.1}$$

and the probability of this event is

$$\begin{aligned} p_{20}^{1} &= Pr\left[2 \le C_N \le M | C_N > 1\right] \\ &= \tfrac{1-(1-P_d)^M - P_d}{1-P_d}. \end{aligned} \tag{B.2}$$

By assuming an ideal routing protocol where spatial relay is negligible, Src can assume that vehicle Z is in the transmission range of the the first car in its cluster, i.e., vehicle Z is approximately C_L + R away from the Src. Finally, the temporal delay in this case is

$$E\left[T_{r_{20}}^{1}\right] \approx \frac{E\left[C_L\right]}{v_e + v_w}. \tag{B.3}$$

i.2) Src is in the same cluster as the original sender or is a member of a large cluster, i.e., a cluster with more than M vehicles. In this case, Src does not have any knowledge about the location of vehicle Z. The re-healing time observed by Src can be approximated by assuming that Src's position will be, on average, in the middle of the S'_{inter} gap. Hence, S'_{inter} should at least be greater than $2R$ and the expected re-healing time in this case can then be approximated as:

$$\begin{aligned} E\left[T_{r_{20}}^{2}\right] &\approx \frac{0.5E\left[S'_{inter} | S'_{inter} > 2R\right] - R}{v_e + v_w} \\ &\approx \frac{1}{2\lambda_w\left(v_e + v_w\right)} \end{aligned}. \tag{B.4}$$

The probability of this event is simply the complement of p_{20}^{1}.

Finally, the expected re-healing time from Src to Z is given by

$$E\left[T_{r_{20}}\right] \approx p_{20}^{1} \times E\left[T_{r_{20}}^{1}\right] + \left(1 - p_{20}^{1}\right) \times E\left[T_{r_{20}}^{2}\right]. \tag{B.5}$$

(ii) **Temporal delay from Z to Dst**: This delay component should be equal to the time elapsed since Z receives the packet till it moves into Dst's transmission range. Since Z receives the packet as soon as it moves into Src's transmission range, the spacing between Z and Dst at the time when Z receives the packet is at least R + the expected inter-cluster spacing. Finally, the delay in this case is given by

$$\begin{aligned} E\left[T_{r_{21}}\right] &\approx \frac{R + E\left[S_{inter}\right] - R}{v_e + v_w} \\ &\approx \frac{R\lambda_e + 1}{\lambda_e\left(v_e + v_w\right)} \end{aligned} \tag{B.6}$$

The total re-healing time or E[T_{r_2}], in this case, is simply

$$E\left[T_{r_2}\right] = E\left[T_{r_{20}}\right] + E\left[T_{r_{21}}\right]. \tag{B.7}$$

Theorem 2 follows by substituting (B.5) and (B.6) into (B.7) and by using Lemma 2 and Lemma 4 in the resulting expression. □

Proof of Corollary 2.1

Follows directly from Theorem 2, by assuming that $\lambda_e R \ll 1$, $\lambda_w R \ll 1$, and by using a first-order Taylor series approximation on the RHS of Eqn. (25) where $e^{-\lambda_e R} \approx 1 - \lambda_e R$ and $e^{-\lambda_w R} \approx 1 - \lambda_w R$. □

APPENDIX C: *Proof of Theorem 3*

Once the packet arrives at the disconnected node, there can be two possible sub-cases which leads to the proof of Theorem 3.

- Case 1: Source can immediately relay packet to one of the vehicles in the opposite direction. The expected re-healing time in this case is given by Theorem 1 and the probability that there is at least one vehicle that is within in the transmission range in the opposite direction is given by the following lemma.

  Lemma 6. *If the inter-vehicle spacing is exponentially distributed with parameter λ_s, the best-case scenario occurs with probability $p_1 = 1 - e^{-2R\lambda_s}$.*

  Proof: *The event that there is no westbound vehicle within a range of 2R happens with probability p_1 which is given by*

$$\begin{aligned} p_1 &= 1 - \frac{(2R\lambda_w)^0}{0!} e^{-2R\lambda_w} \\ &= 1 - e^{-2R\lambda_w} \end{aligned} \tag{C.1}$$

  where λ_w is the westbound traffic density. □

- Case 2: Source *cannot* immediately relay a packet to vehicles in the opposite direction. The expected re-healing time in this case is given by Theorem 2 and the probability of this event happening is given by

$$p_2 = P_{d2} = 1 - p_1 = e^{-2R\lambda_w}. \tag{C.2}$$

Theorem 3 follows from Theorems 1 and 2, Lemma 6, and (C.2). □

Proof of Corollary 3.1:

Follows directly from Proof of Corollary 1.1 and Corollary 2.1. □

REFERENCES

[1] O. K. Tonguz and G. Ferrari, *Ad Hoc Wireless Networks: A Communication-Theoretic Perspective*. John Wiley & Sons, 2006.

[2] N. Wisitpongphan, O. Tonguz, J. Parikh, F. Bai, P. Mudalige, and V. Sadekar, "On the Broadcast Storm Problem in Ad hoc Wireless Network," *IEEE Wireless Communications*, 2007, to appear.

[3] M. Torrent-Moreno, D. Jiang, and H. Hartenstein, "Broadcast reception rates and effects of priority access in 802.11-based vehicular ad-hoc networks," in *Proceedings of ACM International Workshop on Vehicular Ad hoc Networks (VANET 2004)*, Philadelphia, USA, October 2004.

[4] W. Zhao, M. Ammar, and E. Zegura, "A message ferrying approach for data delivery in sparse mobile ad hoc networks," in *Proc. ACM Int. Symp. on Mobile Ad Hoc Network. and Comput.* (MOBIHOC), 2004, pp. 187–198.

[5] N. Wisitpongphan, O. Tonguz, F. Bai, P. Mudalige, and V. Sadekar, "On the Routing Problem in Disconnected Vehicular Networks," in *INFOCOM Minisymposia 2007*, Anchorage, Alaska, USA, May 2007.

[6] D. B. Johnson and D. A. Maltz, "Dynamic source routing in ad hoc wireless networks," in *Mobile Computing*, T. Imielinski and H. Korth, Eds. Kluwer, 1996, pp. 153–181.

[7] X. Hong, T. Kwon, M. Gerla, D. Gu, and G. Pei, "A mobility framework for ad hoc wireless networks," in *ACM 2nd Int'l Conf. on Mobile Data Management (MDM)*, January 2001.

[8] F. Bai, N. Sadagopan, and A. Helmy, "IMPORTANT: A framework to systematically analyze the impact of mobility on performance of routing protocols for adhoc networks," in *Proc. IEEE Conf. on Computer Commun.* (INFOCOM), San Francisco, USA, March 2003, pp. 825–835.

[9] Traffic Flow Theory and Characteristics, US Dept of Transportation Federal Highway Administration, available at http://www.tfhrc.gov/its/tft/toc.pdf.

[10] M. Rickert, K. Nagel, M. Schreckenberg, and A. Latour, "Two lane traffic simulations using cellular automatas," *Physica A*, vol. 231, no. 4, pp. 534–550, 1996.

[11] G. Korkmaz, E. Ekici, F. Ozguner, and U. Ozguner, "Urban Multi-Hop Broadcast Protocol for Inter-Vehicle Communication Systems," in *Proc. of ACM Int'l Workshop on Vehicular Ad hoc Networks (VANET 2004)*, Philadelphia, USA, October 2004, pp. 76–85.

[12] K. Fall, "A delay tolerant networking architecture for challenged internets," in *Proc. ACM SIGCOMM*, August 2003.

[13] D. B. Johnson, D. Maltz, and Y. Hu, "Dynamic source routing protocol for mobile ad hoc networks (dsr)," *IETF Internet Draft*, April 2003, available at http://www3.ietf.org/proceedings/04mar/I-D/draft-ietf-manet-dsr-09.txt.

[14] C. E. Perkins, E. Royer, and S. Das, "Ad hoc on demand distance vector (aodv) routing," *IETF RFC 3561*, July 2003.

[15] S. Jain, K. Fall, and R. Patra, "Routing in a Delay Tolerant Networking," in *Proc. ACM SIGCOMM*, Aug/Sep 2004.

[16] R. C. Shah, S. Roy, S. Jain, and W. Brunette, "Data MULEs: Modeling and analysis of a three-tier architecture for sparse sensor networks," *Elsevier Ad Hoc Networks Journal*, vol. 1/2-3, pp. 215–233, September 2003.

[17] A. Vahdat and D. Becker, "Epidemic routing for partially connected ad hoc networks," Duke University, Tech. Rep., April 2000, cS-200006.

[18] L. Briesemeister and G. Hommel, "Role-based multicast in highly mobile but sparsely connected ad hoc networks," in *Proc. ACM Int. Symp. on Mobile Ad Hoc Network. and Comput.* (MOBIHOC), Boston, USA, August 2000, pp. 45–50.

[19] T. Spyropoulos, K. Psounis, and C. S. Raghavendra, "Single-copy routing in intermittently connected mobile networks," in *The 1st IEEE Comm. Society Conf. SECON'04*, October 2004.

[20] ——, "Spray and wait: An efficient routing scheme for intermittently connected mobile networks," in *WDTN*, 2005.

[21] Z. D. Chen, H. Kung, and D. Vlah, "Ad hoc relay wireless networks over moving vehicles on highways," in *Proc. ACM Int. Symp. on Mobile Ad Hoc Network. and Comput.* (MOBIHOC), Long Beach, CA, USA, 2001, pp. 247–250.

[22] G. Korkmaz, E. Ekici, and F. Ozguner, "An efficient fully ad-hoc multi-hop broadcast protocol for inter-vehicular communication systems," in *Proc. IEEE International Conf. on Commun.* (ICC), Istanbul, Turkey, June 2006.

[23] J. Zhao and G. Cao, "Vadd: Vehicle-assisted data delivery in vehicular ad hoc networks," in *Proc. IEEE Conf. on Computer Commun.* (INFOCOM), 2006.

[24] Highway Capacity Manual 2000, Transportation Research Board (USA).

[25] P. K. Sahoo, S. K. Rao, and V. M. Kumar, "A study of traffic characteristics on two stretches of national highway no 5," *Indian Highways, Indian Road Congress*, vol. 24, no. 4, pp. 11–17, 1996.

[26] Berkeley Highway Lab (BHL), http://bhl.calccit.org/.

[27] O. Tonguz, N. Wisitpongphan, F. Bai, P. Mudalige, and V. Sadekar, "Broadcasting in VANET," in *INFOCOM MOVE Workshop 2007*, Anchorage, Alaska, USA, May 2007.

Nawaporn Wisitpongphan received her B.S. and M.S. degress in electrical and computer engineering from Carnegie Mellon University (CMU), Pittsburgh, PA in 2000 and 2002, respectively. Since 2003, she has been a Research Assistant at Carnegie Mellon University, where she has joined General Motors collaborative research lab and has been working on designing a routing framework for vehicular ad hoc wireless networks (VANET). Her research interests include traffic modeling, self-similarity in Internet, and cross-layer network protocol design for wireless networks. She acts as a frequent reviewer for many international journals and conferences and serves as a technical program committee member for IEEE Conference on Computer Communications (INFOCOM MOVE Workshop) and IEEE International Workshop on Mobile Vehicular Networks (MoVeNet).

Fan Bai is a Senior Researcher in the Electrical & Control Integration Lab., Research & Development Center, General Motors Corporation. Before joining General Motors research lab, he received the B.S. degree in automation engineering from Tsinghua University, Beijing, China, in 1999, and the M.S.E.E. and Ph.D. degrees in electrical engineering, from University of Southern California, Los Angeles, California, U.S.A., in 2005.

His current research is focused on the discovery of fundamental principles and the analysis and design of protocols/systems for next-generation Vehicular Ad hoc Networks(VANET). Dr. Bai has published about 30 conference and journal papers, including INFOCOM, MobiHoc, SECON, IEEE JSAC, IEEE Wireless Communication Magazine and Elsevier AdHoc Networks Journal. He received the **Charles L. McCuen Special Achievement Award** from General Motors Corporation for his research contributions to VANET field in 2006. He also serves as the Technical Program Co-Chair of 1st IEEE International Symposium on Wireless Vehicular Communications (IEEE WiVec 2007).

Priyantha Mudalige is an IEEE member and a chartered professional engineer with eighteen years of industry experience. Currently he is a senior research engineer at General Motors R&D, Warren, Michigan, USA. His research interests include vehicle-to-vehicle and vehicle-to-infrastructure communication based automotive applications, autonomous vehicle navigation and collision avoidance. He is currently the GM technical lead for the Cooperative Intersection Collision Avoidance (CICAS-V) project initiated by the United States Department of Transport (US DOT). He leads several GM internal research activities in the V2V and V2I areas and has been a GM spokesperson for GM V2V communication technology. He has been an active researcher in developing the GM V2V technology and has received several GM awards including the Charles L. McCuen Special Achievement Award in 2006 and the Exceptional Performance Award in the 2005 ITS World Congress V2V demonstrations. Priyantha published about fifteen conference and journal papers in the communications, controls and robotics areas, and has earned 07 US and international patents. He received B.Sc. Eng (Honors) degree from the University of Moratuwa, Sri Lanka in 1987 and M.S. Engineering degree from the University of New South Wales, Australia in 1993.

Varsha Sadekar received her M.S. degree in CSE in 1989 from the Indian Institute of Technology, Bombay and Ph.D. in Systems Engineering in 1997 from Oakland University, MI. Dr. Sadekar has been with General Motors since 1993 and is currently the Manager of the Active Safety and Driver Assistance Systems Group at the R&D Center, Warren, MI. She currently manages several teams involved in the development of active safety applications that provide safety all around the vehicle using combinations of various sensors and algorithms including radar/lidar, computer vision, accurate vehicle positioning, digital road maps, senor/data fusion, and Infrastructure/Vehicle to Vehicle Communications.

Ozan Tonguz received the B.Sc. degree from the University of Essex, England, in 1980, and the M.Sc. and the Ph.D. degrees from Rutgers University, New Brunswick, NJ, in 1986 and 1990, respectively, all in electrical engineering.

He currently serves as a tenured Full Professor in the Department of Electrical and Computer Engineering at Carnegie Mellon University (CMU). Before joining CMU in August 2000, he was with the ECE Dept. of the State University of New York at Buffalo (SUNY/Buffalo). He joined SUNY/Buffalo in 1990 as an Assistant Professor, where he was granted early tenure and promoted to Associate Professor in 1995, and to Full Professor in 1998. Prior to joining academia, he was with Bell Communications Research (Bellcore) between 1988-1990 doing research in optical networks and communication systems. His current research interests are in high-speed networking (Internet), wireless networks and communication systems, optical communications and networks, satellite communications, bioinformatics, and security. He has published over 200 technical papers in IEEE journals and conference proceedings. He is well-known for his contributions in optical networks and wireless communications and networks. His recent work on iCAR (the Integrated Cellular and Ad Hoc Relay Systems) is internationally acclaimed as well (the work has received more than 200 citations in about 4 years). He is the author of the Wiley book (2006) entitled "Ad Hoc Wireless Networks: A Communication-Theoretic Perspective". He was also the architect of the "High Performance Waveform (HPW)" that was implemented in Harris RF Communications' AN/PRC-117f UHF band man-pack tactical radio. His industrial experience includes periods with Bell Communications Research, CTI Inc., Harris RF Communications, Aria Wireless Systems, Clearwire Technologies, Nokia Networks, Nokia Research Center, Neuro Kinetics, Asea Brown Boveri (ABB), General Motors (GM), and Intel. He currently serves or has served as a consultant or expert for several companies (such as Aria Wireless Systems, Harris RF Communications, Clearwire Technologies, Nokia Networks, Alcatel, Lucent Technologies), major law firms, and government agencies in USA, Europe, and Asia in the broad area of telecommunications and networking. He is also a Co-Director (Thrust Leader) of the Center for Wireless and Broadband Networking Research at Carnegie Mellon University. More details about his research interests, research group, projects, and publications can be found at http://www.ece.cmu.edu/∼tonguz/

In addition to serving on the Technical Program Committees of several IEEE conferences (such as INFOCOM, SECON, GLOBECOM, ICC, VTC, WCNC) and symposia in the area of wireless communications and optical networks, Dr. Tonguz currently serves or has served as an Associate Editor for the IEEE TRANSACTIONS ON COMMUNICATIONS, IEEE COMMUNICATIONS MAGAZINE, and IEEE JOURNAL OF LIGHTWAVE TECHNOLOGY. He was a Guest Editor of the special issue of the IEEE JOURNAL OF LIGHTWAVE TECHNOLOGY and IEEE JOURNAL ON SELECTED AREAS IN COMMUNICATIONS on Multiwavelength Optical Networks and Technology, published in 1996, and a Guest Editor of the Special Issue of JOURNAL OF MOBILE MULTIMEDIA on Advanced Mobile Technologies for Health Care Applications (2006).